



MINISTRY OF TECHNOLOGY

LIBRARY AERONAUTICAL RESEARCH COUNCIL  
ROYAL AIRCRAFT ESTABLISHMENT REPORTS AND MEMORANDA  
BEDFORD.

A Numerical Method for Calculating the Pressure  
due to Thickness on Symmetrical Wings at Zero  
Incidence in Supersonic Flow

By R. H. Eldridge and F. Walkden

LONDON: HER MAJESTY'S STATIONERY OFFICE

1968

PRICE £1 2s. 6d. NET

# A Numerical Method for Calculating the Pressure due to Thickness on Symmetrical Wings at Zero Incidence in Supersonic Flow

By R. H. Eldridge and F. Walkden

---

*Reports and Memoranda No. 3535\**  
*September, 1966*

---

## *Summary.*

The equations of motion for supersonic flow over a symmetrical wing at zero incidence are linearised and the pressure coefficient at a point in the wing mean plane is expressed in terms of the finite part of a singular integral. The equation is modified in such a way that the finite part can be calculated analytically, leaving a regular integral to be evaluated numerically. A method of correcting this value of pressure coefficient, to enable an estimate of the value on the wing surface to be made, is discussed. Numerical results for three wings are given and compared with previous results and with experiment.

## CONTENTS

1. Introduction
2. Outline of method
3. Analysis
4. Computation
  - 4.1. Programme
  - 4.2. Wing sections
  - 4.3. Accuracy
  - 4.4. Surface velocity correction
5. Calculated examples:
  - 5.1. Wing 1 – constant chord, 55° swept wing of RAE 101 section
  - 5.2. Wing 2 – tapered, swept wing with a curved tip
  - 5.3. Wing 3 – N.P.L. 55° swept wing of RAE 103 section

Acknowledgements

---

\*Replaces A.R.C. 28 359.

## List of Principal Symbols

### References

Appendix I	Details of the programme and flow diagram
Appendix II	The analysis for regions 2 to 5
Appendix III	Details of the RAE 101 and RAE 103 aerofoil approximations
Table 1	A comparison of values of $C_p$ when using 10 and 20 point Gaussian integration
Table 2	A comparison of exact and calculated values of $C_p$ for a simple chordwise integration
Table 3	A comparison of values of $C_p$ for two different approximations to the thickness distribution
Illustrations	Figs. 1 to 14

### 1. Introduction.

Both in the design of supersonic wings to have a given pressure distribution (Reference 1) and in the calculation of the pressure distribution on an arbitrary cambered wing at incidence, an essential preliminary is to be able to calculate the pressure due to thickness on a symmetrical wing at zero incidence in supersonic flow. To do this exactly is a task that still lies well beyond the capabilities of even the most advanced digital computers, so that it is necessary to have recourse to linearised theory and then to correct the results whenever possible for the principal second order effects. The most important of these occurs in the vicinity of a leading edge that is rounded, but still 'subsonic' in planform with respect to the free stream velocity, and it is then reasonable to suppose that a correction method similar to that commonly used at subsonic speeds will give good results in the supersonic case also.

The present Report describes a numerical method of evaluating the solution to this problem in linearised theory, and suggests a possible form of leading-edge correction.

The principal difficulty in the numerical analysis is to evaluate the finite parts of a number of singular integrals; a computer programme based on the analysis presented in this Report has been written in Algol, and values of the pressure coefficient  $C_p$  at points on various wings have been calculated. The same problem has been considered previously by Haines, Rollins and Osborne (Reference 2), but their numerical techniques are not strictly applicable to wings with rounded leading edges, so that an artifice has to be used to convert the rounded leading-edge shape into an equivalent sharp-edge one. Moreover their method differs from ours in that they calculate the velocity potential at points over the wing and then differentiate numerically to evaluate the velocity field and pressure coefficient.

An appropriate expression for  $C_p$  is derived in Section 2 for the linearised equations of motion. Modifications required in order to evaluate  $C_p$  numerically are described in Section 3. Section 4 contains details of the programme, the way in which the wing geometry must be specified for the programme and a discussion of the accuracy of the calculations. Details of the calculated values of  $C_p$  for three wings are described in Section 5.

### 2. Outline of Method.

We wish to determine the distribution of velocity and pressure on an isolated symmetrical wing with rounded leading edges at zero incidence. Cartesian axes are taken as in Figure 1 so that the mean plane of the wing is  $z = 0$ .

In three-dimensional linearised theory we consider the velocity field

$$\mathbf{U} = U_0(\mathbf{r}_0 + \nabla\phi) \quad (2.1)$$

where  $\mathbf{r}_0$  is the unit vector in the direction of the free stream velocity ( $U_0$ ) and  $\phi$  is the perturbation velocity potential.

Then  $\phi$  satisfies the equation

$$B^2 \frac{\partial^2 \phi}{\partial x^2} - \frac{\partial^2 \phi}{\partial y^2} - \frac{\partial^2 \phi}{\partial z^2} = 0. \quad (2.2)$$

If  $M$  is the free stream Mach number then

$$B^2 = M^2 - 1.$$

Equation (2.2) has a solution of the form (Reference 4)

$$\phi(x,y,z) = -\frac{1}{\pi} \iint_{\Sigma} \frac{\partial z_t(\xi, \eta)}{\partial \xi} \left[ (x-\xi)^2 - B^2 \{(y-\eta)^2 + z^2\} \right]^{-\frac{1}{2}} d\xi d\eta \quad (2.3)$$

where  $z_t(\xi, \eta)$  is the wing thickness distribution and  $\Sigma$  is the area in the plane  $z = 0$  cut off by the forward Mach cone from the point  $(x, y, z)$  (see Figure 1). Equation (2.3) can be written in the form

$$\phi(x,y,z) = -\frac{1}{\pi} \int_{\eta_1(x,y,z)}^{\eta_2(x,y,z)} G(x,y,z,\eta) d\eta \quad (2.4)$$

where

$$G(x,y,z,\eta) = \int_{x_t(\eta)}^{x-B\omega} \frac{\partial z_t(\xi, \eta)}{\partial \xi} \left[ (x-\xi)^2 - B^2 \{(y-\eta)^2 + z^2\} \right]^{-\frac{1}{2}} d\xi, \quad (2.5)$$

$$\omega^2 = (y-\eta)^2 + z^2$$

$\eta_1$  and  $\eta_2$  are the roots of the equation

$$x_t(\eta) = x - B\omega \quad (2.6)$$

and  $x_t(\eta)$  is the  $x$  co-ordinate of the wing leading edge – see Figure 1.

Differentiating (2.4) with respect to  $x$  gives

$$u = \frac{\partial \phi}{\partial x} = -\frac{1}{\pi} \int_{\eta_1}^{\eta_2} \frac{\partial G}{\partial x} d\eta - \frac{1}{\pi} G(x,y,z,\eta_2) \frac{\partial \eta_2}{\partial x} + \frac{1}{\pi} G(x,y,z,\eta_1) \frac{\partial \eta_1}{\partial x} \quad (2.7)$$

Here

$$\begin{aligned} \frac{\partial G}{\partial x} &= \frac{\partial}{\partial x} \int_{x_t(\eta)}^{x-B\omega} \frac{\partial z_t}{\partial \xi} \left[ (x-\xi)^2 - B^2 \{(y-\eta)^2 + z^2\} \right]^{-\frac{1}{2}} d\xi \\ &= -\int_{x_t(\eta)}^{x-B\omega} (x-\xi) \frac{\partial z_t}{\partial \xi} \left[ (x-\xi)^2 - B^2 \{(y-\eta)^2 + z^2\} \right]^{-3/2} d\xi \end{aligned} \quad (2.8)$$

where  $\int$  denotes the finite part of an infinite integral (see Reference 4).

Similar expressions can be found for  $\frac{\partial \phi}{\partial y}$  and  $\frac{\partial \phi}{\partial z}$ .

In this Report we are concerned with wings having rounded leading edges and therefore the streamwise

slope of the wing can be written in the form

$$\frac{\partial z_t}{\partial \xi} = \frac{f(\alpha, \beta)}{\alpha^{\frac{1}{2}}} \quad (2.9)$$

where  $\alpha$  and  $\beta$  are the non-dimensional co-ordinates

$$\alpha = \frac{\xi - sx_t^*(\beta)}{sc(\beta)}, \quad \beta = \eta/s, \quad (2.10)$$

$s$  is the wing semi-span,

$sc(\beta)$  is the local chord, and

$sx_t^*(\beta)$  is the  $x$  co-ordinate of the wing leading edge.

Thus, the radius of curvature at the leading edge ( $R_0$ ) becomes, from (2.9)

$$\frac{R_0(\beta)}{sc(\beta)} = 2 [f(0, \beta)]^2 \quad (2.11)$$

and so near the leading edge,

$$\frac{\partial z_t}{\partial \xi} \sim \left[ \frac{R_0(\beta)}{2(\xi - sx_t^*(\beta))} \right]^{\frac{1}{2}} = \left[ \frac{R_0(\eta/s)}{2(\xi - x_t(\eta))} \right]^{\frac{1}{2}}$$

As  $\eta \rightarrow \eta_1$  or  $\eta \rightarrow \eta_2$ , the integrand of  $G$  becomes infinite and the range of integration becomes zero. Hence we have to obtain the limiting values of  $G$  as  $\eta \rightarrow \eta_1$  and  $\eta \rightarrow \eta_2$ .

$$\lim_{\eta \rightarrow \eta_1} G(x, y, z, \eta) \sim \lim_{\eta \rightarrow \eta_1} \left[ \frac{R_0(\eta/s)}{2} \right]^{\frac{1}{2}} \left[ x - x_t + B\omega \right]^{-\frac{1}{2}} \times \int_{x_t}^{x - B\omega} \frac{d\xi}{(\xi - x_t(\eta))^{\frac{1}{2}} (x - \xi - B\omega)^{\frac{1}{2}}}$$

Now  $\int_a^b \frac{dx}{(x-a)^{\frac{1}{2}}(b-x)^{\frac{1}{2}}} = \pi$  independently of  $a$  and  $b$  and so

$$G(x, y, z, \eta_1) = \frac{1}{2} \pi \left[ \frac{R_0(\eta_1/s)}{x - x_t(\eta_1)} \right]^{\frac{1}{2}} = \frac{1}{2} \pi \left[ \frac{R_0(\beta_1)}{x - sx_t^*(\beta_1)} \right]^{\frac{1}{2}}, \quad (2.12)$$

since  $\eta_1$  is a root of equation (2.6). Similarly

$$G(x, y, z, \eta_2) = \frac{1}{2} \pi \left[ \frac{R_0(\beta_2)}{x - sx_t^*(\beta_2)} \right]^{\frac{1}{2}}$$

Also, from equation (2.6) we have

$$\frac{\partial \eta_1}{\partial x} = - \frac{x - x_t(\eta_1)}{(x - x_t(\eta_1)) \tan \Lambda_{01} + B^2 (y - \eta_1)}, \quad (2.13)$$

where  $\Lambda_{01}$  is the leading edge sweep angle at  $\eta = \eta_1$ ,  $\tan^{-1} \left( \frac{dx_t(\eta_1)}{d\eta} \right)$ .

Similarly 
$$\frac{\partial \eta_2}{\partial x} = \frac{x - x_t(\eta_2)}{(x - x_t(\eta_2)) \tan \Lambda_{02} + B^2 (y - \eta_2)}$$

Putting  $z = 0$ , we obtain from equations (2.7), (2.8), (2.12) and (2.13)

$$\begin{aligned} C_p &= -2 \frac{\partial \phi(x, y, 0)}{\partial x} \\ &= \frac{2}{\pi} \int_{\eta_1}^{\eta_2} H(x, y, \eta) d\eta + \frac{1}{B + \tan \Lambda_{01}} \left[ \frac{R_0(\eta_1/s)}{x - x_t(\eta_1)} \right]^{\frac{1}{2}} \\ &\quad + \frac{1}{B + \tan \Lambda_{02}} \left[ \frac{R_0(\eta_2/s)}{x - x_t(\eta_2)} \right]^{\frac{1}{2}} \end{aligned}$$

where 
$$H(x, y, \eta) = - \int_{x_t(\eta)}^{x - B|\eta - y|} \frac{(x - \xi) \frac{\partial z_t}{\partial \xi} d\xi}{[(x - \xi)^2 - B^2 (\eta - y)^2]^{3/2}} \quad (2.15)$$

The forward Mach cone intersects the wing mean plane in the two straight lines

$$\xi = x \pm B(\eta - y).$$

In general these lines cut off an area which can be divided into five regions (see Figure 2). Regions 3 and 4 disappear for those points  $(x, y)$  through which the Mach lines do not intersect the trailing edge. In this case Region 5 adjoins Region 2.

Now if we express everything in the non-dimensional co-ordinates  $\alpha$  and  $\beta$  we obtain

$$(x, y, 0) \equiv (X, Y, 0)$$

where 
$$X = \frac{x - sx_t^*(Y)}{sc(Y)}, \quad Y = y/s.$$

The Mach lines become

$$\alpha = \alpha_1 \pm \alpha_2,$$

where 
$$\alpha_1 = \frac{1}{c(\beta)} [X c(Y) + x_t^*(Y) - x_t^*(\beta)]$$

and 
$$\alpha_2 = B(\beta - Y)/c(\beta)$$

Thus

$$\begin{aligned} C_p &= -\frac{2}{\pi} \int_{\beta_1}^{\beta_2} \int_0^{x^*} \frac{(\alpha_1 - \alpha) f(\alpha, \beta) d\alpha d\beta}{c(\beta) \alpha^{\frac{1}{2}} (\alpha_1 - \alpha_2 - \alpha)^{3/2} (\alpha_1 + \alpha_2 - \alpha)^{3/2}} \\ &\quad + \frac{1}{B + \tan \Lambda_{01}} \left[ \frac{R_0(\beta_1)}{x - sx_t^*(\beta_1)} \right]^{\frac{1}{2}} + \frac{1}{B + \tan \Lambda_{02}} \\ &\quad \times \left[ \frac{R_0(\beta_2)}{x - sx_t^*(\beta_2)} \right]^{\frac{1}{2}} \end{aligned} \quad (2.16)$$

where  $\alpha^* = \alpha_1 - \alpha_2$  in Region 1  
 $= \alpha_1 + \alpha_2$  in Regions 2 and 5  
 $= 1$  in Regions 3 and 4.

This is a non-dimensional form of equation (19) in Reference 1.

From (2.16) it is possible to calculate  $C_p$ . However, the double integral is not suitable for numerical evaluation in this form as the integrand has a square root singularity at  $\alpha = 0$  and behaves like  $(\alpha_1 \pm \alpha_2 - \alpha)^{-3/2}$  at  $\alpha = \alpha_1 \pm \alpha_2$ . One of the singularities at  $\alpha = \alpha_1 \pm \alpha_2$  always lies outside the range of integration with respect to  $\alpha$  but in the course of the spanwise integration  $\alpha_2 \rightarrow 0$  as  $\beta \rightarrow Y$  and hence  $\alpha_1 - \alpha_2 \sim \alpha_1 + \alpha_2$ . Thus, in this case, as  $\alpha$  approaches the Mach line, these two singularities combine to form a pole of order three.

Before a numerical procedure can be used, it is necessary to remove these singularities from the integrand and evaluate their finite parts analytically, leaving only regular functions to be calculated numerically. The necessary analysis is described in Section 3.

### 3. Analysis.

In this Section we describe a method of converting the double integral in equation (2.16) into a form which is suitable for numerical evaluation. It can be expressed as the sum of a double integral having only square root singularities and a number of single integrals. The analysis will be considered in detail for Region 1 (Figure 2). For the other regions, the analysis is similar and is outlined in Appendix 2

The double integral is replaced by

$$\int_{\beta_1}^{\beta_2} \int_0^{\alpha_1 - x_2} H_1^*(\alpha, \beta) d\alpha d\beta,$$

where

$$\begin{aligned} H_1^*(\alpha, \beta) &= \frac{\alpha_1 - \alpha}{c(\beta) \alpha^{\frac{1}{2}} (\alpha_1 - \alpha_2 - \alpha)^{3/2} (\alpha_1 + \alpha_2 - \alpha)^{3/2}} \\ &\times \left[ f(\alpha, \beta) - f(\alpha_1 - \alpha_2, \beta) \right. \\ &\times \left\{ K_1(\beta) \left( \frac{\alpha}{\alpha_1 - \alpha_2} \right)^{\frac{1}{2}} + K_2(\beta) \left( \frac{\alpha_2}{\alpha_1 - \alpha} \right) \left( \frac{\alpha_1 + \alpha_2 - \alpha}{2\alpha_2} \right)^{3/2} \right\} \\ &\left. - \frac{K_1(\beta) \alpha^{\frac{1}{2}} (\alpha - \alpha_1 + \alpha_2)}{(\alpha_1 - \alpha_2)^{3/2}} \left\{ (\alpha_1 - \alpha_2) f_\alpha(\alpha_1 - \alpha_2, \beta) - \frac{1}{2} f(\alpha_1 - \alpha_2, \beta) \right\} \right] \quad (3.1) \end{aligned}$$

Here  $K_1(\beta)$  and  $K_2(\beta)$  are weighting functions with the following properties:

$$\left. \begin{aligned} K_1(\beta) + K_2(\beta) &= 1, \\ K_1(\beta) (\alpha_1 - \alpha_2)^{-3/2} &\rightarrow 0 \text{ as } \alpha_1 - \alpha_2 \rightarrow 0, \\ K_1(\beta) &\rightarrow 1 \text{ as } \alpha_2 \rightarrow 0, \\ K_2(\beta) \alpha_2^{-\frac{1}{2}} &\rightarrow 0 \text{ as } \alpha_2 \rightarrow 0, \\ K_2(\beta) &\rightarrow 1 \text{ as } \alpha_1 - \alpha_2 \rightarrow 0. \end{aligned} \right\} \quad (3.2)$$

and

$H_1^*(\alpha, \beta)$  is the integrand of (2.16) except for certain terms that have been subtracted in order to ensure that it contains only integrable singularities in the region of integration. These terms have been chosen so that they can be integrated analytically with respect to  $\alpha$ .

We shall show that  $H_1^*(\alpha, \beta)$  is regular in Region 1 except when  $\alpha = 0$  or  $\alpha = \alpha_1 - \alpha_2$ , where it has square root singularities. Consider the chordwise integration at the general section  $\beta = \beta^*$ . As  $\alpha \rightarrow \alpha_1 - \alpha_2$ ,

$$H_1^*(\alpha, \beta^*) \sim \frac{\alpha_1 - \alpha}{c(\beta^*) \alpha^{\frac{1}{2}} (\alpha_1 - \alpha_2 - \alpha)^{3/2} (\alpha_1 + \alpha_2 - \alpha)^{3/2}} \left[ f(\alpha, \beta^*) - f(\alpha_1 - \alpha_2, \beta^*) \right. \\ \times \left\{ K_1(\beta^*) + K_2(\beta^*) \right\} - \frac{K_1(\beta^*) \alpha^{\frac{1}{2}} (\alpha - \alpha_1 + \alpha_2)}{(\alpha_1 - \alpha_2)^{3/2}} \\ \left. \times \left\{ (\alpha_1 - \alpha_2) f_\alpha(\alpha_1 - \alpha_2, \beta^*) - \frac{1}{2} f(\alpha_1 - \alpha_2, \beta^*) \right\} \right]$$

Since  $K_1(\beta^*) + K_2(\beta^*) = 1$ ,

$$K_1(\beta^*) (\alpha_1 - \alpha_2)^{-3/2} \rightarrow 0 \text{ as } \alpha_1 - \alpha_2 \rightarrow 0$$

and  $f(\alpha, \beta^*) - f(\alpha_1 - \alpha_2, \beta^*)$  is  $O(\alpha - \alpha_1 + \alpha_2)$

it can be seen that  $H_1^*(\alpha, \beta^*)$  is regular apart from a square root singularity at  $\alpha = \alpha_1 - \alpha_2$ .

It is necessary also to consider two special cases. As  $\beta^* \rightarrow M[1]$  (i.e. the  $\beta$  co-ordinate of the intersection of the Mach line and the leading edge),  $\alpha_1 - \alpha_2 \rightarrow 0$ ,  $K_1(\beta^*) (\alpha_1 - \alpha_2)^{-3/2} \rightarrow 0$  and  $K_2(\beta^*) \rightarrow 1$ . Then

$$H_1^*(\alpha, \beta^*) \sim \frac{\alpha_1 - \alpha}{c(\beta^*) \alpha^{\frac{1}{2}} (\alpha_1 - \alpha_2 - \alpha)^{3/2} (\alpha_1 + \alpha_2 - \alpha)^{3/2}} \left[ f(\alpha, \beta^*) - f(\alpha_1 - \alpha_2, \beta^*) \right],$$

as  $\alpha \rightarrow \alpha_1 - \alpha_2$  and it can be seen that  $H_1^*(\alpha, \beta^*)$  is regular apart from a square root singularity at  $\alpha = \alpha_1 - \alpha_2$ .

Also as  $\beta^* \rightarrow Y$ ,  $\alpha_2 \rightarrow 0$ ,  $K_2(\beta^*) \alpha_2^{-\frac{1}{2}} \rightarrow 0$  and  $K_1(\beta^*) \rightarrow 1$ . Then as  $\alpha \rightarrow \alpha_1 - \alpha_2$ ,

$$H_1^*(\alpha, \beta^*) \sim \frac{\alpha_1 - \alpha}{c(\beta^*) (\alpha_1 - \alpha)^3} \left[ \frac{f(\alpha, \beta^*)}{\alpha^{\frac{1}{2}}} - \frac{f(\alpha_1 - \alpha_2, \beta^*)}{\alpha^{\frac{1}{2}}} \left( \frac{\alpha}{\alpha_1 - \alpha_2} \right)^{\frac{1}{2}} \right. \\ \left. - (\alpha - \alpha_1 + \alpha_2) \left\{ \frac{f_\alpha(\alpha_1 - \alpha_2, \beta^*)}{(\alpha_1 - \alpha_2)^{\frac{1}{2}}} - \frac{1}{2} \frac{f(\alpha_1 - \alpha_2, \beta^*)}{(\alpha_1 - \alpha_2)^{3/2}} \right\} \right]$$

The expression in square brackets is  $O[(\alpha - \alpha_1 + \alpha_2)^2]$  and so in this case  $H_1^*(\alpha, \beta^*)$  is regular at  $\alpha = \alpha_1 - \alpha_2$ .

The weighting factors  $K_1(\beta)$  and  $K_2(\beta)$  are necessary because the functions subtracted from the integrand to give it the required behaviour near  $\beta = Y$  are singular at  $\beta = M[1]$  and *vice versa*.

A transformation can be defined which maps the square root singularity onto a point outside the range of integration. Consider the integral

$$\int_0^{\alpha_1 - \alpha_2} \frac{d\alpha}{\alpha^{\frac{1}{2}} (\alpha_1 - \alpha_2 - \alpha)^{\frac{1}{2}}},$$

and make the transformation

$$\alpha = 0.25 (\alpha_1 - \alpha_2) (1 + \zeta)^2 (2 - \zeta). \quad (3.3)$$



Then the integral becomes

$$\int_{-1}^1 \frac{3 d \zeta}{(4-\zeta^2)^{\frac{3}{2}}}$$

and the integrand is regular in the range of integration.

Applying this transformation to

$$\int_0^{\alpha_1-\alpha_2} H_1^*(\alpha, \beta) d \alpha,$$

we obtain

$$\int_{-1}^1 \frac{3(\alpha_1-\alpha) F_1(\alpha, \beta) d \zeta}{c(\beta)(4-\zeta^2)^{\frac{3}{2}}(\alpha_1-\alpha_2-\alpha)(\alpha_1+\alpha_2-\alpha)^{3/2}} \quad (3.4)$$

where

$$F_1(\alpha, \beta) = f(\alpha, \beta) - f(\alpha_1 - \alpha_2, \beta) \left\{ K_1 \left( \frac{\alpha}{\alpha_1 - \alpha_2} \right)^{\frac{1}{2}} + K_2 \left( \frac{\alpha_2}{\alpha_1 - \alpha} \right) \left( \frac{\alpha_1 + \alpha_2 - \alpha}{2 \alpha_2} \right)^{3/2} \right\} \\ - \frac{K_1 \alpha^{\frac{1}{2}} (\alpha - \alpha_1 + \alpha_2)}{(\alpha_1 - \alpha_2)^{3/2}} \left\{ (\alpha_1 - \alpha_2) f_\alpha(\alpha_1 - \alpha_2, \beta) - \frac{1}{2} f(\alpha_1 - \alpha_2, \beta) \right\}. \quad (3.5)$$

Now the double integral  $\int_{\beta_1}^{\beta_2} \int_0^{\alpha_1-\alpha_2} H_1^*(\alpha, \beta) d \alpha d \beta$  can be evaluated numerically provided that the method used does not require the value of  $H_1^*(\alpha, \beta)$  at points where  $\alpha = \alpha_1 - \alpha_2$ . At these points, although  $H_1^*(\alpha, \beta)$  is regular it is numerically indeterminate because both numerator and denominator are zero. We use a Gaussian integration formula which overcomes this difficulty because it does not use the end points of the range of integration.

The contribution from Region 1 to the integral of (2.16) can be expressed in the form

$$I_1 = - \int_{\beta_1}^{\beta_2} \int_{-1}^1 \frac{3(\alpha_1-\alpha) F_1(\alpha, \beta) d \zeta d \beta}{c(\beta)(4-\zeta^2)^{\frac{3}{2}}(\alpha_1-\alpha_2-\alpha)(\alpha_1+\alpha_2-\alpha)^{3/2}} \\ - \int_{\beta_1}^{\beta_2} \int_0^{\alpha_1-\alpha_2} \frac{K_1(\beta)(\alpha_1-\alpha_2)f(\alpha_1-\alpha_2, \beta) d \alpha d \beta}{c(\beta)(\alpha_1-\alpha_2)^{\frac{1}{2}}(\alpha_1-\alpha_2-\alpha)^{3/2}(\alpha_1+\alpha_2-\alpha)^{3/2}} \\ - \int_{\beta_1}^{\beta_2} \int_0^{\alpha_1-\alpha_2} \frac{K_2(\beta)\alpha_2 f(\alpha_1-\alpha_2, \beta) d \alpha d \beta}{c(\beta)\alpha^{\frac{1}{2}}(\alpha_1-\alpha_2-\alpha)^{3/2}(2\alpha_2)^{3/2}} \\ + \int_{\beta_1}^{\beta_2} \int_0^{\alpha_1-\alpha_2} \frac{K_1(\beta)(\alpha_1-\alpha_2)[(\alpha_1-\alpha_2)f_\alpha(\alpha_1-\alpha_2, \beta) - \frac{1}{2}f(\alpha_1-\alpha_2, \beta)] d \alpha d \beta}{c(\beta)(\alpha_1-\alpha_2)^{3/2}(\alpha_1-\alpha_2-\alpha)^{\frac{1}{2}}(\alpha_1+\alpha_2-\alpha)^{3/2}}$$

where  $\beta_1 = Y$  and  $\beta_2 = M[1]$ .

It can be shown that

$$\int_0^{\alpha_1 - \alpha_2} \frac{(\alpha_1 - \alpha) d\alpha}{(\alpha_1 - \alpha_2 - \alpha)^{3/2} (\alpha_1 + \alpha_2 - \alpha)^{3/2}} = -\frac{1}{(\alpha_1^2 - \alpha_2^2)^{3/2}}$$

$$\int_0^{\alpha_1 - \alpha_2} \frac{(\alpha_1 - \alpha) d\alpha}{(\alpha_1 - \alpha_2 - \alpha)^{3/2} (\alpha_1 + \alpha_2 - \alpha)^{3/2}} = \log \frac{[(\alpha_1 - \alpha_2)^{3/2} + (\alpha_1 + \alpha_2)^{3/2}]^2}{2\alpha_2} - \left(\frac{\alpha_1 - \alpha_2}{\alpha_1 + \alpha_2}\right)^{3/2},$$

and 
$$\int_0^{\alpha_1 - \alpha_2} \frac{d\alpha}{\alpha^{3/2} (\alpha_1 - \alpha_2 - \alpha)^{3/2}} = 0$$

Hence

$$I_1 = -\int_{\beta_1}^{\beta_2} \int_{-1}^1 \frac{3(\alpha_1 - \alpha) F_1(\alpha, \beta) d\zeta d\beta}{c(\beta) (4 - \zeta^2)^{3/2} (\alpha_1 - \alpha_2 - \alpha) (\alpha_1 + \alpha_2 - \alpha)^{3/2}}$$

$$+ \int_{\beta_1}^{\beta_2} \frac{K_1 f(\alpha_1 - \alpha_2, \beta) d\beta}{c(\beta) (\alpha_1 - \alpha_2) (\alpha_1 + \alpha_2)^{3/2}} + \int_{\beta_1}^{\beta_2} \frac{K_1}{c(\beta) (\alpha_1 - \alpha_2)^{3/2}} \left\{ (\alpha_1 - \alpha_2) f_\alpha(\alpha_1 - \alpha_2, \beta) \right.$$

$$\left. - \frac{1}{2} f(\alpha_1 - \alpha_2, \beta) \right\} \times \left\{ \log \frac{[(\alpha_1 - \alpha_2)^{3/2} + (\alpha_1 + \alpha_2)^{3/2}]^2}{2\alpha_2} \right.$$

$$\left. - \left(\frac{\alpha_1 - \alpha_2}{\alpha_1 + \alpha_2}\right)^{3/2} \right\} d\beta. \quad (3.6)$$

The last integral in (3.6) has a logarithmic singularity at  $\alpha_2 = 0$  ( $\alpha_2 \rightarrow 0$  as  $\beta \rightarrow Y$ ).

This is treated by rewriting the integral in the following way:

$$\int_{\beta_1}^{\beta_2} \frac{K_1}{c(\beta) (\alpha_1 - \alpha_2)^{3/2}} \left\{ (\alpha_1 - \alpha_2) f_\alpha(\alpha_1 - \alpha_2, \beta) - \frac{1}{2} f(\alpha_1 - \alpha_2, \beta) \right\}$$

$$\times \left\{ 2 \log \left( (\alpha_1 - \alpha_2)^{3/2} + (\alpha_1 + \alpha_2)^{3/2} \right) - \left(\frac{\alpha_1 - \alpha_2}{\alpha_1 + \alpha_2}\right)^{3/2} \right\} d\beta$$

$$- \int_{\beta_1}^{\beta_2} \left\{ \frac{K_1}{c(\beta) (\alpha_1 - \alpha_2)^{3/2}} \left[ (\alpha_1 - \alpha_2) f_\alpha(\alpha_1 - \alpha_2, \beta) - \frac{1}{2} f(\alpha_1 - \alpha_2, \beta) \right] - \frac{1}{c(Y) X^{3/2}} \right.$$

$$\left. \times \left[ X f_\alpha(X, Y) - \frac{1}{2} f(X, Y) \right] \right\} \log 2\alpha_2 d\beta$$

$$- \frac{1}{c(Y) X^{3/2}} \left[ X f_\alpha(X, Y) - \frac{1}{2} f(X, Y) \right] \left\{ \int_{\beta_1}^{\beta_2} \log \frac{2B}{c(\beta)} d\beta + \left[ (\beta - Y) \log(\beta - Y) - \beta \right]_{\beta_1}^{\beta_2} \right\}.$$

The second integrand in the above expression  $\sim \alpha_2 \log 2\alpha_2$  as  $\alpha_2 \rightarrow 0$  and so is regular.

Thus, we obtain

$$\begin{aligned}
I_1 = & - \int_{\beta_1}^{\beta_2} \int_{-1}^1 \frac{3(\alpha_1 - \alpha) F_1(\alpha, \beta) d\zeta d\beta}{c(\beta) (4 - \zeta^2)^{\frac{1}{2}} (\alpha_1 - \alpha_2 - \alpha) (\alpha_1 + \alpha_2 - \alpha)^{3/2}} \\
& + \int_{\beta_1}^{\beta_2} \frac{K_1 f(\alpha_1 - \alpha_2, \beta) d\beta}{c(\beta) (\alpha_1 - \alpha_2) (\alpha_1 + \alpha_2)^{\frac{1}{2}}} \\
& + \int_{\beta_1}^{\beta_2} \frac{K_1}{c(\beta) (\alpha_1 - \alpha_2)^{3/2}} \left\{ (\alpha_1 - \alpha_2) f_\alpha(\alpha_1 - \alpha_2, \beta) - \frac{1}{2} f(\alpha_1 - \alpha_2, \beta) \right\} \\
& \quad \left\{ 2 \log \left[ (\alpha_1 + \alpha_2)^{\frac{1}{2}} + (\alpha_1 - \alpha_2)^{\frac{1}{2}} \right] - \left( \frac{\alpha_1 - \alpha_2}{\alpha_1 + \alpha_2} \right)^{\frac{1}{2}} \right\} d\beta \\
& - \int_{\beta_1}^{\beta_2} \left\{ \frac{K_1}{c(\beta) (\alpha_1 - \alpha_2)^{3/2}} \left[ (\alpha_1 - \alpha_2) f_\alpha(\alpha_1 - \alpha_2, \beta) - \frac{1}{2} f(\alpha_1 - \alpha_2, \beta) \right] - \frac{1}{c(Y) X^{3/2}} \right. \\
& \quad \left. \times \left[ X f_\alpha(X, Y) - \frac{1}{2} f(X, Y) \right] \right\} \log 2 \alpha_2 d\beta \\
& - \frac{1}{c(Y) X^{3/2}} \left[ X f_\alpha(X, Y) - \frac{1}{2} f(X, Y) \right] \left\{ \int_{\beta_1}^{\beta_2} \log \frac{2B}{c(\beta)} d\beta + \left[ (\beta - Y) \log(\beta - Y) - \beta \right]_{\beta_1}^{\beta_2} \right\}. \tag{3.7}
\end{aligned}$$

For Region 1, the contribution to the integral of (2.16) can be evaluated from (3.7) where  $\zeta$  is defined by (3.3) and  $F_1(\alpha, \beta)$  by (3.5). The formulae used to calculate the contribution from the remaining regions are given in Appendix 2.

Finally, we note that the calculated value of  $C_p$  is at a point in the wing mean plane, whereas in an experiment the value measured would be that on the surface. This means that some correction should be made to the calculated results before direct comparison with experiment is made. This problem is discussed in Section 4.4 of this Report.

## 4. Computation.

### 4.1. The Programme.

The computer programme has been written in Algol and developed using an English Electric KDF 9 computer. A flow diagram of the programme and details of the input information required appear in Appendix 1.

The integrations are performed using Gaussian Integration formulae and the coefficients for both the 10 point and 20 point formulae are built into the programme. In each region the double integral is evaluated as a repeated integral in which integration in the  $\alpha$  direction is followed by integration in the  $\beta$  direction. Clearly if the 10 point formula is used, the integrand has to be evaluated at 100 points in each region.

With the Kidsgrove Algol fast compiler using the Gaussian 10 point integration formula, the time taken to calculate  $C_p$  at a point involving only Regions 1, 2 and 5 is approximately 15 seconds and for a point involving all five regions approximately 25 seconds is needed.

### 4.2. Wing Sections.

In this Report we consider wings having rounded leading edges. The wing slope in the free stream direction can be expressed in the form, equation (2.9),

$$\frac{\partial z_t}{\partial x} = \alpha^{-\frac{1}{2}} f(\alpha, \beta)$$

With  $\frac{\partial z_t}{\partial x}$  defined in this way, we obtain

$$z_t = sc(\beta) g(\alpha, \beta),$$

where

$$g(\alpha, \beta) = \int_0^\alpha \alpha^{-\frac{1}{2}} f(\alpha, \beta) d\alpha.$$

If the thickness-chord ratio of the wing sections at different chord stations is constant, then  $f(\alpha, \beta)$  will be independent of  $\beta$  and all wing sections will have the same slope at points where the lines  $\alpha = \text{constant}$  cut them.

A large class of wings have 'similar' sections and for these,  $f(\alpha, \beta)$  can be expressed in the form

$$f(\alpha, \beta) = f_1(\alpha) f_2(\beta).$$

The polynomial  $f_2(\beta)$  defines the variation of thickness-chord ratio along the span. The three wings considered in this Report have 'similar' sections; two based on the RAE 101 aerofoil and one based on the RAE 103 aerofoil. In the programme, the function  $f_1(\alpha)$  may be expressed either in the form

$$(i) \quad f_1(\alpha) = \sum_{i=0}^N a_i \alpha^i$$

$$\text{or (ii)} \quad f_1(\alpha) = a_{-1} + \alpha^{\frac{1}{2}} \sum_{i=0}^N a_i \alpha^i.$$

For more general wings, the programme is arranged so that  $f(\alpha, \beta)$  is specified by a function of  $\alpha$  for a number of values of  $\beta$  and an interpolation procedure is used to calculate  $f(\alpha, \beta)$  at intermediate values of  $\beta$ . The position and number of these  $\beta$ -points where  $f(\alpha, \beta)$  is defined, may be specified arbitrarily.

In our calculations,  $f_1(\alpha)$  is an approximation to  $\alpha^{\frac{1}{2}} \frac{\partial z_t}{\partial x}$  and can be derived from values of  $\frac{\partial z_t}{\partial x}$  at discrete points, by standard curve fitting procedures. Polynomial representations of type (i) have been calculated for the RAE 101, and 103 aerofoils using the method of least squares. The coefficients are given in Appendix 3. It was found impossible to cover the whole range  $0 \leq \alpha \leq 1$  accurately with a single polynomial, so a number of polynomials are used. These have been arranged so that together they define a curve which is a piecewise continuous approximation to the given aerofoil. In general,  $f_\alpha(\alpha, \beta)$  will be discontinuous at points where the curves represented by the polynomials join. However, it is unlikely that these discontinuities will have a significant effect on the calculation because  $f_\alpha(\alpha, \beta)$  is evaluated at only a few points on either the Mach lines or the trailing edge of the wing. Also the Gaussian integration has the effect of smoothing out any discontinuities in the integrand. Nevertheless, it would seem desirable to have the smallest number of polynomials consistent with an approximation of given accuracy.

In order to assess the effect of the choice of polynomial representation of thickness on the calculation, an alternative set of polynomials was used for the RAE 101 aerofoil and values of  $C_p$  on Wing 1 calculated again. The two sets of results are compared in Table 3 and are within 1 per cent of each other for most points.

#### 4.3. Accuracy.

For a general wing, the overall accuracy of the calculation is difficult to assess. In theory, the range of integration can be continually subdivided until any required order of accuracy is achieved, but this

would require such a large amount of computing time that it is impracticable.

The computed results for Wing 1 agree satisfactorily with the analytical results obtained by Weber (Reference 2). Further, the results obtained by the method described in this Report have been compared with experimental results available for the wings considered in Section 5. We conclude that the overall accuracy of our calculation is satisfactory in the cases we have considered and since there is no reason to suppose that the accuracy of the calculation will be significantly different for other wing shapes, we believe that the method described here will produce satisfactory results in general.

The accuracy of the evaluation of the single integrals and the integration in the chordwise direction of the double integrals can be checked by any simple integration procedure in which the interval is progressively subdivided until the results converge. Wherever it seemed necessary, this checking procedure has been carried out using a Simpson integration formula and is described in Section 5.

In addition, a check on the accuracy of the chordwise integration has been carried out for the case of a parabolic wing section ( $f(\alpha, \beta) = 1$ ) which allows an exact solution of the integral in terms of complete elliptic integrals (Reference 3).

From equation (2.16), we have for the chordwise integration in Region 1,

$$I = - \int_0^{\alpha_1 - \alpha_2} \frac{(\alpha_1 - \alpha) f(\alpha, \beta) d\alpha}{c(\beta) \alpha^{\frac{1}{2}} (\alpha_1 - \alpha_2 - \alpha)^{3/2} (\alpha_1 + \alpha_2 - \alpha)^{3/2}}$$

Integrating by parts gives,

$$I = \text{finite part} \left[ \frac{f(\alpha, \beta)}{c(\beta) \alpha^{\frac{1}{2}}} (\alpha_1 - \alpha_2 - \alpha)^{-\frac{1}{2}} (\alpha_1 + \alpha_2 - \alpha)^{-\frac{1}{2}} \right]_0^{\alpha_1 - \alpha_2} \\ - \int_0^{\alpha_1 - \alpha_2} \frac{\alpha f_{\alpha}(\alpha, \beta) - \frac{1}{2} f(\alpha, \beta)}{c(\beta) \alpha^{3/2} (\alpha_1 - \alpha_2 - \alpha)^{\frac{1}{2}} (\alpha_1 + \alpha_2 - \alpha)^{\frac{1}{2}}} d\alpha$$

The term in square brackets is infinite at both limits and so the finite part is zero. Putting  $f(\alpha, \beta) = 1$  gives

$$I = \frac{1}{2 c(\beta)} \int_0^{\alpha_1 - \alpha_2} \frac{d\alpha}{\alpha^{3/2} (\alpha_1 - \alpha_2 - \alpha)^{\frac{1}{2}} (\alpha_1 + \alpha_2 - \alpha)^{\frac{1}{2}}}$$

This integral can be expressed in elliptic integrals. It can be shown (see Reference 5, Section 234.04) that

$$\int_x^{\alpha_1} \frac{d\alpha}{\alpha^{3/2} (\alpha_1 - \alpha_2 - \alpha)^{\frac{1}{2}} (\alpha_1 + \alpha_2 - \alpha)^{\frac{1}{2}}} = \frac{2}{(\alpha_1 - \alpha_2)(\alpha_1 + \alpha_2)^{\frac{1}{2}}} \int_0^{u_1} dc^2 u du,$$

for  $\alpha > 0$

where  $sn^2 u_1 = \frac{(\alpha_1 + \alpha_2)(\alpha_1 - \alpha_2 - \alpha)}{(\alpha_1 - \alpha_2)(\alpha_1 + \alpha_2 - \alpha)}$

and modulus  $k = \left( \frac{\alpha_1 - \alpha_2}{\alpha_1 + \alpha_2} \right)^{\frac{1}{2}}$

Also  $\int_0^{u_1} dc^2 u du = F(\phi, k) - E(\phi, k) + dn u_1 \operatorname{tn} u_1$ ,

where  $\sin \phi = sn u_1$

Thus, in the limit  $\alpha \rightarrow 0$  ( $\phi \rightarrow \pi/2$ ), the last term is infinite and the finite part has the value  $(K(k) - E(k))$  where  $K(k)$  and  $E(k)$  are the complete elliptic integrals. Hence

$$I = -\frac{1}{c(\beta)} \frac{1}{(\alpha_1 - \alpha_2)(\alpha_1 - \alpha_2)^{\frac{1}{2}}} \left[ E(k) - K(k) \right]$$

If we write 
$$\delta = \frac{\alpha_2}{\alpha_1} = \frac{B(\beta - Y)}{X c(Y) + x_1^*(Y) - x_1^*(\beta)},$$

then 
$$I^* = -c(\beta) \alpha_1^{3/2} I = \frac{E(k) - K(k)}{(1 - \delta)(1 + \delta)^{\frac{1}{2}}},$$

and 
$$k = \left( \frac{1 - \delta}{1 + \delta} \right)^{\frac{1}{2}}.$$

In Legendre's notation, writing  $k = \sin \theta$  then gives

$$\delta = \frac{1 - \sin^2 \theta}{1 + \sin^2 \theta}.$$

We are particularly interested in the chordwise integration near the point  $(X, Y)$  where the singularities on the two Mach lines combine i.e. small values of  $\delta$  ( $\theta \sim \pi/2$ ). Values of  $I^*$  for  $\theta = 85^\circ, 87^\circ, 88^\circ, 89^\circ$  are given in Table 2.

Now we have to express equation (3.7) in a similar form. Putting  $f(\alpha, \beta) = 1$ ,  $f_x(\alpha, \beta) = 0$ ,  $K_1 = 1$ ,  $K_2 = 0$ ,  $\alpha = \alpha_1 \gamma$  and  $\alpha_2/\alpha_1 = \delta$  then gives for the chordwise integration,

$$\begin{aligned} I^* &= -c(\beta) \alpha_1^{3/2} I = \int_{-1}^1 \frac{3(1 - \gamma)}{(4 - \zeta^2)^{\frac{1}{2}} (1 - \delta - \gamma)(1 + \delta - \gamma)^{3/2}} \\ &\times \left[ 1 - \left( \frac{\gamma}{1 - \delta} \right)^{\frac{1}{2}} + \frac{1}{2} \frac{\gamma^{\frac{1}{2}} (\gamma - 1 + \delta)}{(1 - \delta)^{3/2}} \right] d\zeta - \frac{1.5}{(1 - \delta)(1 + \delta)^{\frac{1}{2}}} \\ &+ \frac{1}{2(1 - \delta)^{3/2}} \log \frac{[(1 - \delta)^{\frac{1}{2}} + (1 + \delta)^{\frac{1}{2}}]^2}{2\delta}, \end{aligned}$$

where 
$$\gamma = \frac{1 - \delta}{4} (2 + 3\zeta - \zeta^3).$$

$I^*$  has been calculated from this equation using Gaussian 10 point integration and compared with the exact solution in Table 2. It can be seen that our numerical calculation for this simple case is extremely accurate.

#### 4.4. Surface Velocity Correction.

It is well known that simple linearised theory—in which the boundary conditions are applied and the velocity calculated, both in the mean plane of the wing—is invalid near a rounded leading edge however thin the wing may be. It is necessary therefore to make some form of leading-edge correction. There are a number of equally plausible possibilities; the one suggested below is based on the proposals of Haines *et al* (Reference 2), which is equivalent in concept to the 'Riegels rule' used in subsonic two-dimensional calculations. At the same time it is convenient to make some allowance for the lateral component of velocity

$$v_y = U_0 \frac{\partial \phi}{\partial y}.$$

Although this makes only a second order contribution to the total velocity on the wing surface, it is known that improved accuracy can often be obtained by including a rough approximation for it.

Suppose that the perturbation velocity vector  $(v_x, v_y)$  in the plane  $z = 0$  has been calculated using linearised theory. The resultant velocity makes an angle  $\psi = \tan^{-1} (-v_y/v_x)$  with the  $x$ -axis. Define new axes  $\xi, \eta$  in this direction and perpendicular to it. The velocity components along these axes then become

$$V_\xi = U_0 \cos \psi + v_x \sec \psi$$

$$V_\eta = U_0 \sin \psi.$$

Now we assume (by analogy with two-dimensional subsonic theory) that in going from the plane  $z = 0$  to the wing surface, the component  $V_\eta$  is unchanged, but the component  $V_\xi$  is multiplied by the factor

$$\left[ 1 + \left( \frac{\partial z_t}{\partial \xi} \right)^2 \right]^{-\frac{1}{2}}$$

where  $\frac{\partial z_t}{\partial \xi} = \frac{\partial z_t}{\partial x} \cos \psi - \frac{\partial z_t}{\partial y} \sin \psi$ , the wing slope in the  $\xi$  direction. Thus  $V_\xi$  becomes replaced by

$$V'_\xi = V_\xi \left[ 1 + \left( \frac{\partial z_t}{\partial \xi} \right)^2 \right]^{-\frac{1}{2}},$$

and hence the total velocity  $V'$  is given by

$$(V')^2 = U_0^2 \sin^2 \psi + \frac{V_\xi^2}{1 + \left( \frac{\partial z_t}{\partial \xi} \right)^2}.$$

Now define  $\theta$  by

$$\tan \theta = -\frac{\partial z_t}{\partial y} / \frac{\partial z_t}{\partial x}$$

so that for an untapered wing  $\theta$  is equal to the sweep angle  $\Lambda$ . Then

$$\frac{\partial z_t}{\partial \xi} = \frac{\partial z_t}{\partial x} \frac{\cos(\theta - \psi)}{\cos \theta}$$

and hence

$$\left( \frac{V'}{U_0} \right)^2 = \sin^2 \psi + \frac{(\cos \psi + \frac{v_x}{U_0} \sec \psi)^2}{1 + \left( \frac{\partial z_t}{\partial x} \right)^2 \cos^2(\theta - \psi) \sec^2 \theta}$$

This can now be used with the exact pressure-velocity relation, to calculate  $C_p'$  (the corrected value of  $C_p$ ), where

$$C_p' = \frac{2}{\gamma M^2} \left\{ \left( 1 + \frac{\gamma-1}{2} M^2 \left[ 1 - \left( \frac{V'}{U_0} \right)^2 \right] \right)^{\frac{\gamma}{\gamma-1}} - 1 \right\} \quad (4.1)$$

Here  $M$  is the free stream Mach number and  $\gamma$  is the ratio of the specific heats of air (approximately 1.4). The above equation reduces, in linearised theory to

$$C_p' = -2 \frac{v_x}{U_0} = -2 \frac{\partial \phi}{\partial x}$$

but it is probably better to use the exact equation when possible.

This analysis requires the knowledge of both  $v_x$  and  $v_y$ , but our computer programme is designed to calculate only  $v_x$ . Although  $v_y$  could be calculated in a similar manner, the computing time required would be increased significantly. We feel that the extra effort needed to obtain values of  $v_y$  is not really worthwhile.

Accordingly, the simplifying assumption is made that, except near the root or tip,  $\psi = \theta = \Lambda$ , the local angle of sweep. For an untapered wing,  $\Lambda$  is just the leading (and trailing) edge sweep angle, but for a tapered wing it is less obvious what value should be taken. Since the main effect of the correction is near the leading edge, it is desirable that at least  $\Lambda$  should take its local value ( $\tan^{-1} dx_t/dy$ ) there. We therefore suggest defining  $\Lambda$  by

$$\tan \Lambda = \frac{dx_t}{dy} + \frac{x-x_t}{c} \frac{dc}{dy},$$

thus allowing  $\Lambda$  to vary along the chord in an appropriate manner.

We must also allow for the fact that  $v_y$  is zero at the root (and probably also at the tips) of the wing. This can be done crudely by following the analogy of the corresponding subsonic theory (Reference 6), in which  $\Lambda$  is replaced by  $\Lambda^*$ , defined by

$$\Lambda^* = (1-K)\Lambda,$$

where  $K$  is a function of  $y$ . For want of any other evidence we define  $K$  as in subsonic theory by

$$K = K_r + K_t,$$

$$\text{where } K_r = \frac{0.068 - 0.122(y/c_r)}{0.068 + y/c_r} \text{ for } y/c_r < 0.557$$

$$= 0 \text{ for } y/c_r \geq 0.557$$

$$\text{and } K_t = \frac{0.073 - 0.098 \frac{s-y}{c_t}}{0.104 + \frac{s-y}{c_t}} \text{ for } \frac{s-y}{c_t} < 0.745$$

$$= 0 \quad \text{for } \frac{s-y}{c_t} \geq 0.745.$$



Here  $c_r$  is the root chord and  $c_t$  is a representative tip chord. For a tapered wing, use the actual tip chord or 0.1 times the root chord, whichever is the larger. For a planform having a curved edge at the tip, this representative tip chord may be taken as 0.4 times the chord at  $y/s = 0.75$ .

With this definition of  $\Lambda^*$  we then have

$$\left(\frac{V'}{U_0}\right)^2 = \sin^2 \Lambda^* + \frac{(\cos \Lambda^* + \frac{v_x}{U_0} \sec \Lambda^*)^2}{1 + \left(\frac{\partial z_t}{\partial x}\right)^2 \sec^2 \Lambda^*} \quad (4.2)$$

• which, when inserted in equation (4.1), gives the value of  $C_p$ . At the root ( $\beta = 0$ ) this reduces to

$$\left(\frac{V'}{U_0}\right)^2 = \frac{\left(1 + \frac{v_x}{U_0}\right)^2}{1 + \left(\frac{\partial z_t}{\partial x}\right)^2},$$

as it should.

Alternatively, in view of what is known about the leading edge correction in subsonic flow (Reference 6), it may be preferable to replace  $\frac{\partial z_t}{\partial x}$  by

$$\frac{\partial z_t}{\partial x} (1 - M^2 \cos^2 \Lambda_0)^{-\frac{1}{2}}.$$

Here we have used  $\Lambda_0$  (the leading-edge sweep angle) in place of  $\Lambda^*$  to avoid the possibility of  $1 - M^2 \cos^2 \Lambda$  becoming negative near the root or tips.

This gives

$$\left(\frac{V'}{U_0}\right)^2 = \sin^2 \Lambda^* + \frac{(\cos \Lambda^* + \frac{v_x}{U_0} \sec \Lambda^*)^2}{1 + \left(\frac{\partial z_t}{\partial x}\right)^2 \frac{\sec^2 \Lambda^*}{1 - M^2 \cos^2 \Lambda_0}} \quad (4.3)$$

which when inserted in equation (4.1) gives the value of  $C_p$ .

It should be noted that for highly swept wings of the type we consider, since  $v_y \cong v_x \tan \Lambda$ , then  $v_y$  may be numerically greater than  $v_x$ . Thus it is not justifiable to ignore  $v_y/U_0$  unless we also ignore  $(v_x/U_0)$ . Hence it is not appropriate to use equations 8a and 8b of Reference 2.

## 5. Calculated Examples.

### 5.1. Wing 1 - Constant Chord, 55° Swept Wing of RAE 101 Section.

This wing (wing A of Reference 2) is shown in Figure 3. It was chosen so that a comparison of our numerical results could be made with the analytical results of Weber and the numerical results of Haines, Rollins and Osborne. However, the wing that we use has the true rounded leading edge of the RAE 101 aerofoil, whereas the results obtained by Haines *et al* and Weber are for a sharp leading edge approximation to the RAE 101 aerofoil. Some disagreement in the results near the leading edge is therefore to be expected. The results are compared in Figure 4.

On the centreline ( $Y = 0$ ), apart from near the leading edge, there is good agreement: and the same is true at  $Y = 0.25$  aft of about  $X = 0.3$ . The discrepancies near the leading edge are of course consistent

with the difference in the shapes of the assumed sections, as explained in the previous paragraph.

A detailed investigation of the numerical calculation for this wing has been made. The results obtained by using the 10 point and the 20 point Gaussian integration formulae are compared in Table 1. The values obtained with the 10 point integration formula are within 2 per cent of those obtained using the 20 point integration formula for most points and the extra time needed to carry out the calculation using the 20 point formula does not seem to be justified in general.

The point (0.9, 0.3), where the difference is 9 per cent of the (small) value given by the 20 point formula, was chosen for closer study. A detailed print out of all stages of the calculation was obtained and graphs of the various integrands were examined. A selection of these graphs are shown in Figures 5a, b, c and d. It was found that most of the curves were smooth and well behaved like those in Figures 5a and b. The results obtained by the Gaussian and Simpson integration procedures agreed very closely. Even in the worst case, Figure 5d, the difference was only 6 per cent of a small quantity, for the 10 point integration formula. In Figures 5c and d the violent oscillations that occur are caused by discontinuities in  $f_x(\alpha, \beta)$  where two polynomials join (see Section 4.2).

### 5.2. Wing 2 – Tapered, Swept Wing with a Curved Tip.

The planform of this wing (Wing B in Reference 2) is shown in Figure 6. The leading edge was approximated by the following polynomials.

$$0 \leq \eta \leq 0.5417, \quad x_i(\eta) = 1.68085\eta.$$

$$0.5417 \leq \eta \leq 1, \quad x_i(\eta) = -14.6769 + 71.4511\eta - 109.9240\eta^2 + 57.5232\eta^3.$$

The results are compared with those of Haines *et al* in Figure 7.

### 5.3. Wing 3 – N.P.L. 55° swept wing of RAE 103 section.

The planform of this wing is shown in Figure 8. The leading edge was approximated by the following polynomials.

$$0 \leq \eta \leq 4.2013, \quad x_i(\eta) = 1.428148\eta$$

$$4.2013 \leq \eta \leq 9.4207, \quad x_i(\eta) = 2252.205702 - 2947.567216\eta + 1672.146280\eta^2 \\ - 536.267867\eta^3 + 106.396215\eta^4 - 13.373899\eta^5 + 1.040336\eta^6 \\ - 0.45801\eta^7 + 0.000874\eta^8$$

$$9.4207 \leq \eta \leq 9.5158, \quad x_i(\eta) = 19324.89767 - 4093.739369\eta + 217.004967\eta^2$$

A half-model of this wing has been extensively tested in the 20 in. square transonic tunnel at the N.P.L.; a comparison of experimental and calculated pressure distributions at four spanwise positions is shown in Figures 9 to 12 for a range of Mach numbers from 1.1 to 1.4. Near the root ( $y/s = 0.22$ ) the agreement is good at all Mach numbers, and also at the tip ( $y/s = 0.88$ ) at  $M = 1.1$  and 1.2. Even at these Mach numbers the calculations slightly underestimate the peak velocity in the middle of the half wing ( $y/s = 0.66$ ), and at higher speeds a shock wave appears and moves outward and rearward as the Mach number increases; and under these circumstances there is naturally poorer agreement between theory and experiment. Bearing this in mind the overall picture seems reasonably satisfactory, although there is insufficient evidence to assess the relative merits of the two leading-edge corrections, equations (4.2) and (4.3).

### Acknowledgments.

This work has been carried out under a Ministry of Technology research contract and the authors

acknowledge the support that they have received from the Ministry.

They are also indebted to Dr. R. C. Lock of the N.P.L. for providing details of the experimental results and to the Computing Staff of the University of Salford for their co-operation in testing and running the programme.



## LIST OF PRINCIPAL SYMBOLS

$B =$	$(M^2 - 1)^{\frac{1}{2}}$ , <i>see</i> equation (2.2)
$c(\beta)$	The length of the chord at the point $(\alpha, \beta)$
$C_p$	The pressure coefficient at a point
$C_p'$	A corrected value of $C_p$ for a point on the wing surface
$C_{p1}$	The corrected value of $C_p$ using equation (4.2)
$C_{p2}$	The corrected value of $C_p$ using equation (4.3)
$f(\alpha, \beta)$	A function used in evaluating the wing slope, <i>see</i> equation (2.9)
$f_1$	<i>See</i> equations (A1.2) and (A1.3)
$f_2$	<i>See</i> equation (A1.1)
$f_\alpha =$	$\frac{\partial f(\alpha, \beta)}{\partial \alpha}$
$F_1(\alpha, \beta)$	<i>See</i> equation (3.5)
$G(x, y, z, \eta)$	<i>See</i> equation (2.5)
$H(x, y, \eta)$	<i>See</i> equation (2.15)
$H_1^*(\alpha, \beta)$	<i>See</i> equation (3.1)
$I, I^*$	Expressions for integrals appearing in Section 4.3
$I_1$	The contribution from Region 1 to the integral in equation (2.16)
$K_1, K_2$	Weighting functions defined by equations (3.2)
$M$	Free-stream Mach number
$M[1], M[2]$	The $\beta$ co-ordinates of the intersections of the Mach lines with the leading edge
$N[1], N[2]$	The $\beta$ co-ordinates of the intersections of the Mach lines with the trailing edge
$r_0$	Unit vector in free-stream direction
$R_0$	Radius of curvature at the leading edge, <i>see</i> equation (2.11)
$s$	Semi-span of wing
$u$	Perturbation velocity component in streamwise direction
$U$	Velocity vector
$U_0$	Magnitude of free-stream velocity
$v$	Perturbation velocity component in spanwise direction
$v_x =$	$u$
$v_y =$	$v$
$V_\xi, V_\eta, V', V_\xi$	<i>See</i> Section 4.4
$x$	Co-ordinate in streamwise direction
$X$	Non-dimensional $x$ co-ordinate

$x_i(\eta) = sx_i^*(\beta)$	x co-ordinate of leading edge
$y$	Co-ordinate in spanwise direction
$Y$	Non-dimensional $y$ co-ordinate
$z$	Co-ordinate in vertical direction
$z_i(x,y)$	Half-wing thickness at point $(x,y)$
$\alpha$	Non-dimensional co-ordinate in streamwise direction. <i>See equation (2.10)</i>
$\alpha_1 =$	$1/c(\beta) [Xc(Y) + x_i^*(Y) - x_i^*(\beta)]$
$\alpha_2 =$	$B(\beta - Y)/c(\beta)$
$\beta$	Non-dimensional co-ordinate in spanwise direction
$\beta_1, \beta_2$	Limits of integration in spanwise direction
$\beta^*$	A particular value of $\beta$
$\gamma$	Ratio of specific heats (1.4)
$\theta =$	$\tan^{-1} \left( -\frac{\partial z_i}{\partial y} / \frac{\partial z_i}{\partial x} \right)$
$\phi$	Perturbation velocity potential
$\psi =$	$\tan^{-1} (-v_y/v_x)$
$\Lambda$	Angle of sweep
$\Lambda_{01}$	Leading-edge sweep angle at $\beta = M[1]$
$\Lambda_{02}$	Leading-edge sweep angle at $\beta = M[2]$
$\Sigma$	Area of integration
$\xi$	Dummy variable of integration in $x$ direction
$\eta$	Dummy variable of integration in $y$ direction
$\eta_1, \eta_2$	Roots of equation (2.6)
$\zeta$	Transformation variable, <i>see equation (3.3)</i>
$\omega =$	$\left[ (y - \eta)^2 + z^2 \right]^{1/2}$

---

## REFERENCES

- | <i>No.</i> | <i>Author(s)</i>                                 | <i>Title, etc.</i>   |
|------------|--|--|
| 1          | R. C. Lock and<br>J. Bridgewater .. ..           | A method for the aerodynamic design of the wings and fuselage for swept wing aircraft intended to cruise at transonic and supersonic speeds.<br>N.P.L. Aero Report 1096, March, 1964.                          |
| 2          | A. B. Haines, K. Rollins<br>and J. Osborne .. .. | The calculation of the velocity distribution due to thickness for swept wings with subsonic edges at supersonic speeds.<br>A.R.C. C.P. 654, June 1962.   |
| 3          | R. C. Lock .. ..                                 | Notes on the numerical evaluation of the pressure due to thickness, according to linearised theory.<br>Unpublished N.P.L. Aero Note.   |
| 4          | W. R. Sears (editor) .. ..                       | General theory of high speed aerodynamics. Vol. 6 in <i>High speed aerodynamics and jet propulsion</i> . Princeton, 1955.  |
| 5          | P. F. Byrd and .. ..<br>M. O. Friedman           | <i>Handbook of Elliptic Integrals</i> .<br>Springer Verlag, 1954.  |
| 6          |  | Method for predicting the pressure distribution on swept wings with subsonic attached flow.<br><i>R.Aeronaut.Soc.</i> Transonic Data Memorandum 6312, December 1963.<br>Amendments and addenda, February 1965. |
-

## APPENDIX I

### *Details of the Programme.*

#### 1. *Wing Geometry.*

##### (a) *Leading Edge.*

A polynomial approximation to the leading edge is used in the programme. A procedure  $l(\eta)$  is used to evaluate  $\xi$  at a point on the leading edge corresponding to a given value of  $\eta$ . In practice there may be more than one polynomial to cover the range  $0 \leq \eta \leq s$ . The curve defined by the polynomial is a representation of the leading edge in cartesian co-ordinates  $(\xi, \eta)$  with axes as shown in Figure 1. The coefficients of the polynomial are automatically adjusted within the programme for use with the non-dimensional co-ordinates  $(\alpha, \beta)$ . The input information required to define the leading edge is:

$n1$ , the number of polynomials defining different sections of the leading edge,

$m1$ , the degree of the polynomial of highest order,

$b1[i]$ , the  $\eta$  co-ordinates of the points at which the curves represented by the polynomials join,  $i = 1, 2, \dots, n1 - 1$ . If  $n1 = 1$ , then no values are supplied.

$A1[i,0] \dots A1[i,m1]$ , the coefficients of the  $i$ 'th polynomial,  $i = 1, 2, \dots, n1$ .

Then

$$\xi = x_i(\eta) = \sum_{j=0}^{m1} A1[i,j] \eta^j, \quad i = 1, 2, \dots, n1.$$

It should be noted that if any of the polynomials is of degree  $p < m1$  then the coefficients of  $\eta^k$  where  $k = p + 1, p + 2, \dots, m1$  must be read in as zero.

##### (b) *Trailing Edge.*

The trailing edge is defined in a similar way to the leading edge and the value of  $\xi$  at a point on the trailing edge corresponding to a given value of  $\eta$  is calculated using a procedure  $tr(\eta)$ . The input information required to define the trailing edge is:

$n2$ , the number of polynomials defining different sections of the trailing edge,

$m2$ , the degree of the polynomial of highest order,

$b2[i]$ , the  $\eta$  co-ordinate of the points at which the curves represented by the polynomials join,  $i = 1, 2, \dots, n2 - 1$ . If  $n2 = 1$ , then no values are supplied.

$A2[i,0] \dots A2[i,m2]$  - the coefficients of the  $i$ 'th polynomial.

Then

$$\xi = tr(\eta) = \sum_{j=0}^{m2} A2[i,j] \eta^j, \quad i = 1, 2, \dots, n2.$$

##### (c) *Chord.*

The length of chord at a point  $\eta$  is calculated using a procedure  $c(\eta)$  where

$$c(\eta) = tr(\eta) - l(\eta).$$

##### (d) *Wing Slope.*

As explained in Section 4.2, we use for the wing slope the expression

$$\frac{\partial z_t}{\partial x} = \alpha^{-\frac{1}{2}} f(\alpha, \beta) = \alpha^{-\frac{1}{2}} f_1(\alpha) f_2(\beta).$$

In the programme we define  $f_2(\beta)$  so that

$$f_2(\beta) = \sum_{k=0}^{m4} A4[i,k] \beta^k \quad (A1.1)$$

and we define  $f_1(\alpha)$  so that either

$$f_1(\alpha) = \sum_{k=0}^{m3} A3[i,j,k] \alpha^k, \quad (A1.2)$$

or

$$f_1(\alpha) = A3[i,j,-1] + \alpha^{\frac{1}{2}} \sum_{k=0}^{m3} A3[i,j,k] \alpha^k, \quad (A1.3)$$

where

$$i = 1, 2, \dots, n3 \text{ and } j = 1, 2, \dots, n4.$$

In order to obtain accurate representations of a wide variety of surfaces, the programme has been arranged so that different parts of the wing planform can have the slope represented by different functions. The wing planform is divided into  $n4$  areas by the lines

$$\beta = \text{constant} = b4[i], i = 1, 2, \dots, n4 - 1$$

and then each of these areas is subdivided into  $n3$  sub-areas by the lines

$$\alpha = \text{constant} = b3[i,j], j = 1, 2, \dots, n3 - 1.$$

giving a total of  $n3 \times n4$  sub-areas. For each sub-area (defined by  $i$  and  $j$ ) the coefficients  $A3[i,j,k]$ , where  $k = 0, 1, \dots, m3$  must be given so that values of  $f_1(\alpha)$  may be calculated. If equation (A1.3) is used to evaluate  $f_1(\alpha)$  then an extra coefficient  $A3[i,j,-1]$  is required. For each area (defined by the parameter  $i$ ) the coefficients  $A4[i,k]$  where  $k = 0, 1, \dots, m4$  must be given so that values of  $f_2(\beta)$  may be calculated. In practice not all the areas defined by the lines  $\beta = b4[i]$  may need to be subdivided into  $n3$  sub-areas. Suppose area  $p$  needs subdividing into  $q$  sub-areas where  $q < n3$ . Then we put  $b3[p,j] = 1$  for  $q \leq j \leq n3$  and the coefficients  $A3[p,j,k]$  associated with the sub-areas for which  $q < j \leq n3$  are made equal to zero. These coefficients are never used but are required by the input procedure. An example of how a wing planform might be divided up is shown in Figure 13. For the wings described in Section 5 only one area was ever used.

In the programme two integers  $S1[i]$  and  $S2[i]$  are associated with each of the areas defined by the lines  $\beta = b4[i]$ . These integers are chosen by the user and act as switches within the programme. If the wing sections within the area are 'similar', then  $S1[i]$  must be positive and in this case the wing slope will be calculated using  $f_1(\alpha) f_2(\beta)$  at the point  $(\alpha, \beta)$ . If  $S1[i]$  is made negative, then the wing slope will be calculated by interpolating between the values of  $f_1(\alpha) f_2(\beta)$  at the points  $(\alpha, b4[i-1])$  and  $(\alpha, b4[i])$ . If  $S2[i]$  is made positive, then  $f_1(\alpha)$  is calculated using equation (A1.1) and if  $S2[i]$  is made negative, then  $f_1(\alpha)$  is calculated using equation (A1.2).

The input information required to define the wing slope is:

$n3$ , the maximum number of sub-areas within an area,



$n4$ ,	the number of areas of wing planform,
$m3$ ,	the degree of the polynomial of highest order associated with $f_1(\alpha)$ in a sub-area,
$m4$ ,	the degree of the polynomial of highest order representing $f_2(\beta)$ in an area,
$b3[i,j]$ ,	the $\alpha$ co-ordinates of points where the sub-areas adjoin ( <i>see</i> notes above),
$b4[i]$ ,	the $\beta$ co-ordinates of points where the areas adjoin - if only one area then no value is supplied,
$S1[i]$ ,	switch, integer determining whether interpolation is used to calculate the value of wing slope,
$S2[i]$ ,	switch, integer determining whether $f_1(\alpha)$ is calculated from equation (A1.1) or equation (A1.2).
$A3[i,j,k]$ ,	coefficients of $f_1(\alpha)$ in each sub-area
$A4[i,k]$ ,	coefficients of $f_2(\beta)$ in each area

## 2. Other Procedures.

### (a) Mach Lines.

The value of  $\alpha$  on the Mach lines, corresponding to a given value of  $\beta$  is evaluated using the procedures  $P1(\beta)$  and  $P2(\beta)$  where

$$P1(\beta) = \alpha_1(\beta) - \alpha_2(\beta)$$

and

$$P2(\beta) = \alpha_1(\beta) + \alpha_2(\beta).$$

The expressions  $\alpha_1(\beta)$  and  $\alpha_2(\beta)$  are defined in Section 2 of this Report.

### (b) Weighting functions.

The weighting functions  $K1(\beta)$  and  $K2(\beta)$  have the properties described in (3.2). In the programme  $K1(\beta)$  is defined as follows

$$K1(\beta) = 10t^3 - 15t^4 + 6t^5$$

where

$$t = (M[1] - \beta) / (M[1] - Y) \quad \text{in Region 1,}$$

$$t = (\beta - M[2]) / (N[2] - M[2]) \quad \text{in Region 5.}$$

and  $t = 1$  in all other regions

A typical graph of  $K1(\beta)$  is shown in Figure 14.

### (c) Intersection.

In the non-dimensional co-ordinates  $(\alpha, \beta)$  the leading edge is given by  $\alpha = 0$  and the trailing edge by  $\alpha = 1$ . The procedure intersection calculates the values  $\beta = M[1]$  and  $\beta = M[2]$  where the Mach lines intersect the leading edge. It also tests to see whether the Mach lines intersect the trailing edge and if they do, it then calculates the values  $\beta = N[1]$  and  $\beta = N[2]$ .

### (d) Integration procedures.

These procedures calculate the integrand of the various integrals in equation (3.7), for use in the Gaussian integration formula. The modified Gaussian points are evaluated using the relations

$$\int_a^b f(x) dx = \frac{1}{2}(b-a) \int_{-1}^1 f^*(y) dy$$

$$= \frac{1}{2}(b-a) \sum_{j=1}^n G_j f^*(g_j)$$

$$= \frac{1}{2}(b-a) \sum_{j=1}^n G_j f(e_j)$$

where

$$f(x) = f^*(y),$$

$$x = \frac{1}{2}[(b-a)y + a + b],$$

$G_j$  are the Gaussian weight factors

and  $g_j$  are the Gaussian points.

Then the modified Gaussian points are

$$e_j = \frac{1}{2}[(b-a)g_j + a + b]$$

#### INPUT DATA

<i>Programme Symbol</i>	<i>Explanation</i>
$z$	An integer representing the output device on the computer (line printer = 30)
$S3$	The number of Gaussian points used (either 10 or 20)
$n1$	The number of polynomials defining sections of the leading edge
$n2$	The number of polynomials defining different sections of the trailing edge
$n3$	The maximum number of sub-areas within a region of the wing planform
$n4$	The number of areas of wing planform
$m1$	The degree of the leading-edge polynomial of highest order
$m2$	The degree of the trailing-edge polynomial of highest order
$m3$	The degree of the polynomial of highest order associated with $f_1(x)$ in a sub-area
$m4$	The degree of the polynomial of highest order representing $f_2(\beta)$ in an area
$b$	The value of the wing semi-span
$B$	$(M^2 - 1)^{\frac{1}{2}}$ , where $M$ is the Mach number of the free stream
$W$	The number of points at which $C_p$ is required
$b1[1]$ $\vdots$ $b1[n1-1]$	The co-ordinates of points at which the leading-edge polynomials change. If $n1 = 1$ then no values are supplied

*Programme Symbol*

*Explanation*

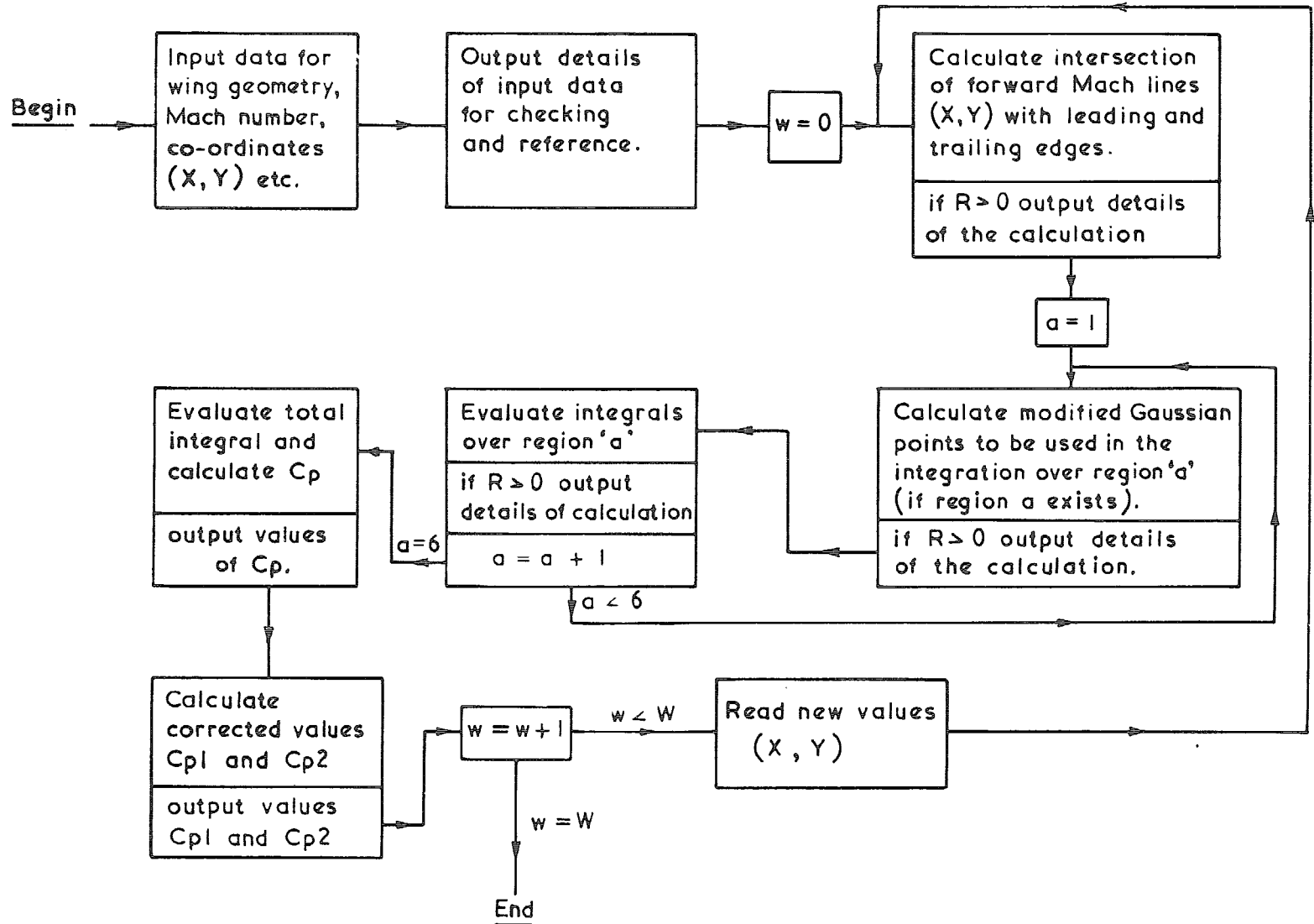
$\left. \begin{array}{c} b2[1] \\ \vdots \\ b2[n2-1] \end{array} \right\}$	<p>The co-ordinates of points at which the trailing-edge polynomials change. If <math>n2 = 1</math> then no values are supplied</p>
$\left. \begin{array}{c} b3[1,1] \\ \vdots \\ b3[1,n3-1] \end{array} \right\}$	<p>The <math>\alpha</math> co-ordinates of points at which the functions representing <math>f_1(\alpha)</math> change in area 1 (see Appendix 1 Section 1(d))</p>
$\left. \begin{array}{c} b3[n4,1] \\ \vdots \\ b3[n4,n3-1] \end{array} \right\}$	<p>The <math>\alpha</math> co-ordinates of points at which the functions representing <math>f_1(\alpha)</math> change in area <math>n4</math>. These points define the limits of each sub-area</p>
$\left. \begin{array}{c} b4[1] \\ \vdots \\ b4[n4-1] \end{array} \right\}$	<p>The <math>\beta</math> co-ordinates of points at which the functions representing <math>f_2(\beta)</math> change. These points define the limits of each area</p>
$\left. \begin{array}{c} S1[1] \\ \vdots \\ S1[n4] \end{array} \right\}$	<p>Switch for each area. If <math>S1[i]</math> is positive then polynomial evaluation of <math>f(\alpha,\beta)</math> in area <math>i</math>. If <math>S1[i]</math> is negative then interpolation</p>
$\left. \begin{array}{c} S2[1] \\ \vdots \\ S2[n4] \end{array} \right\}$	<p>Switch for each area. If <math>S2[i]</math> is positive then <math>f_1(\alpha)</math> is calculated from (A1.2) in area <math>i</math>. If <math>S2[i]</math> is negative then <math>f_1(\alpha)</math> is calculated from (A1.3)</p>
$\left. \begin{array}{c} A1[1,0] \\ \vdots \\ A1[1,m1] \end{array} \right\}$	<p>The coefficients of the leading-edge polynomial in the first section of the leading edge</p>
$\left. \begin{array}{c} A1[n1,0] \\ \vdots \\ A1[n1,m1] \end{array} \right\}$	<p>The coefficients of the leading-edge polynomial in the <math>n1</math> section of leading edge</p>
$\left. \begin{array}{c} A2[1,0] \\ \vdots \\ A2[1,m2] \end{array} \right\}$	<p>The coefficients of the trailing edge polynomial in the first section of the trailing edge</p>
$\left. \begin{array}{c} A2[n2,0] \\ \vdots \\ A2[n2,m2] \end{array} \right\}$	<p>The coefficients of the trailing edge polynomial in the <math>n2</math> section of the trailing edge</p>
$\left. \begin{array}{c} A3[1,1,-1] \\ A3[1,1,0] \\ \vdots \\ A3[1,1,m3] \end{array} \right\}$	<p>The coefficients of <math>f_1(\alpha)</math> in sub-area (1,1)</p>
$\left. \begin{array}{c} A3[1,n3,-1] \\ A3[1,n3,0] \\ \vdots \\ A3[1,n3,m3] \end{array} \right\}$	<p>The coefficients of <math>f_1(\alpha)</math> in sub-area (1,<math>n3</math>)</p>
$\left. \begin{array}{c} A4[1,0] \\ \vdots \\ A4[1,m4] \end{array} \right\}$	<p>The coefficients of <math>f_2(\beta)</math> in area 1</p>

$\left. \begin{array}{l} A3[n4,1-1] \\ A3[n4,1,0] \\ \vdots \\ A3[n4,1,m3] \\ \vdots \\ A3[n4,n3,-1] \\ A3[n4,n3,0] \\ \vdots \\ A3[n4,n4,m3] \end{array} \right\}$	<p>The coefficients of <math>f_1(\alpha)</math> in sub-area <math>(n4,1)</math></p> <p>The coefficients of <math>f_1(\alpha)</math> in sub-area <math>(n4, n3)</math></p>
$\left. \begin{array}{l} A4[n4,0] \\ \vdots \\ A4[n4,m4] \end{array} \right\}$	<p>The coefficients of <math>f_2(\beta)</math> in area <math>n4</math></p>

$R$  Switch. If  $R$  is positive then all intermediate steps of the calculation are output.  
 If  $R$  is negative then no intermediate steps are output

$\left. \begin{array}{l} X \\ Y \\ \vdots \\ \vdots \\ \vdots \\ X \\ Y \end{array} \right\}$	<p><math>W</math> values of <math>(\alpha,\beta)</math> where the value of <math>C_p</math> is required</p>
---	---

Chapter flow diagram for calculation of pressure coefficient



## APPENDIX II

In this Appendix we describe the analysis for Regions 2 to 5. For Regions 2 and 5 the analysis is the same.

$$\begin{aligned}
 I_{2,5} = & - \int_{\beta_1}^{\beta_2} \int_{-1}^1 \frac{3(\alpha_1 - \alpha) F_{2,5}(\alpha, \beta) d\zeta d\beta}{c(\beta) (4 - \zeta^2)^{\frac{1}{2}} (\alpha_1 - \alpha_2 - \alpha)^{3/2} (\alpha_1 + \alpha_2 - \alpha)} + \int_{\beta_1}^{\beta_2} \frac{K_1 f(\alpha_1 + \alpha_2, \beta) d\beta}{c(\beta) (\alpha_1 + \alpha_2) (\alpha_1 - \alpha_2)^{\frac{1}{2}}} \\
 & + \int_{\beta_1}^{\beta_2} \frac{K_1}{c(\beta) (\alpha_1 + \alpha_2)^{3/2}} \left[ (\alpha_1 + \alpha_2) f_\alpha(\alpha_1 + \alpha_2, \beta) - \frac{1}{2} f(\alpha_1 + \alpha_2, \beta) \right] \\
 & \quad \times \left[ 2 \log \left( (\alpha_1 + \alpha_2)^{\frac{1}{2}} + (\alpha_1 - \alpha_2)^{\frac{1}{2}} \right) - \left( \frac{\alpha_1 + \alpha_2}{\alpha_1 - \alpha_2} \right)^{\frac{1}{2}} \right] d\beta \\
 & - \int_{\beta_1}^{\beta_2} \left\{ \frac{K_1}{c(\beta) (\alpha_1 + \alpha_2)^{3/2}} \left[ (\alpha_1 + \alpha_2) f_\alpha(\alpha_1 + \alpha_2, \beta) - \frac{1}{2} f(\alpha_1 + \alpha_2, \beta) \right] - \frac{1}{c(Y) X^{3/2}} \right. \\
 & \quad \left. \times \left[ X f_\alpha(X, Y) - \frac{1}{2} f(X, Y) \right] \right\} \log 2\alpha_2 d\beta \\
 & - \frac{1}{c(Y) X^{3/2}} \left[ X f_\alpha(X, Y) - \frac{1}{2} f(X, Y) \right] \left\{ \int_{\beta_1}^{\beta_2} \log \frac{2B}{c(\beta)} d\beta - \left[ (Y - \beta) \log(Y - \beta) + \beta \right] \right\}_{\beta_1}^{\beta_2}
 \end{aligned} \tag{A2.1}$$

where

$$\begin{aligned}
 F_{2,5}(\alpha, \beta) = & f(\alpha, \beta) - f(\alpha_1 + \alpha_2, \beta) \left\{ K_1 \left( \frac{\alpha}{\alpha_1 + \alpha_2} \right)^{\frac{1}{2}} + K_2 \left( \frac{-\alpha_2}{\alpha_1 - \alpha} \right) \left( \frac{\alpha_1 - \alpha_2 - \alpha}{-2\alpha_2} \right)^{3/2} \right\} \\
 & - K_1 \frac{\alpha^{\frac{1}{2}}}{(\alpha_1 + \alpha_2)^{\frac{1}{2}}} (\alpha - \alpha_1 - \alpha_2) \left\{ (\alpha_1 + \alpha_2) f_\alpha(\alpha_1 + \alpha_2, \beta) - \frac{1}{2} f(\alpha_1 + \alpha_2, \beta) \right\}
 \end{aligned} \tag{A2.2}$$

and

$$\alpha = \frac{\alpha_1 + \alpha_2}{4} (2 + 3\zeta - \zeta^3). \tag{A2.3}$$

For Region 2:

$$\beta_1 = N[1], \quad \beta_2 = Y.$$

For Region 5:

$$\beta_1 = M[2], \quad \beta_2 = N[2].$$

For Regions 3 and 4 three modifications have to be made. Firstly, the integrals in the chordwise direction have the range of integration 0 to 1. Secondly, in these regions  $\alpha_1 + \alpha_2$  is never zero and so we can make  $K_1(\beta) = 1$  and  $K_2(\beta) = 0$ . Thirdly, we have to replace  $f(\alpha_1 + \alpha_2, \beta)$  by  $f(1, \beta)$  since now  $\alpha_1 + \alpha_2 > 1$  and so  $f(\alpha_1 + \alpha_2, \beta)$  is no longer defined.

Then

$$\begin{aligned}
I_{3,4} = & - \int_{\beta_1}^{\beta_2} \int_0^1 \frac{(\alpha_1 - \alpha) F_{3,4}(\alpha, \beta) d\alpha d\beta}{c(\beta) \alpha^{\frac{1}{2}} (\alpha_1 - \alpha_2 - \alpha)^{3/2} (\alpha_1 + \alpha_2 - \alpha)^{3/2}} - \int_{\beta_1}^{\beta_2} \frac{f(1, \beta) d\beta}{c(\beta) (\alpha_1 + \alpha_2 - 1)^{\frac{1}{2}} (\alpha_1 - \alpha_2 - 1)^{\frac{1}{2}}} \\
& + \int_{\beta_1}^{\beta_2} \frac{f(1, \beta) d\beta}{c(\beta) (\alpha_1 + \alpha_2)^{\frac{1}{2}} (\alpha_1 - \alpha_2)^{\frac{1}{2}}} \\
& + \int_{\beta_1}^{\beta_2} \frac{1}{c(\beta)} \left( f_{\alpha}(1, \beta) - \frac{1}{2} f(1, \beta) \right) \left[ \left( \frac{\alpha_1 + \alpha_2 - 1}{\alpha_1 - \alpha_2 - 1} \right)^{\frac{1}{2}} - \left( \frac{\alpha_1 + \alpha_2}{\alpha_1 - \alpha_2} \right)^{\frac{1}{2}} \right. \\
& \left. + 2 \log \left( \frac{(\alpha_1 - \alpha_2)^{\frac{1}{2}} + (\alpha_1 + \alpha_2)^{\frac{1}{2}}}{(\alpha_1 - \alpha_2 - 1)^{\frac{1}{2}} + (\alpha_1 + \alpha_2 - 1)^{\frac{1}{2}}} \right) \right] d\beta
\end{aligned} \tag{A2.4}$$

where

$$F_{3,4}(\alpha, \beta) = f(\alpha, \beta) - \alpha^{\frac{1}{2}} f(1, \beta) - \alpha^{\frac{1}{2}} (\alpha - \alpha_1 - \alpha_2) \left\{ f_{\alpha}(1, \beta) - \frac{1}{2} f(1, \beta) \right\} \tag{A2.5}$$

Here we have used the results

$$\int_0^1 \frac{(\alpha_1 - \alpha) d\alpha}{(\alpha_1 - \alpha_2 - \alpha)^{3/2} (\alpha_1 + \alpha_2 - \alpha)^{3/2}} = \frac{1}{(\alpha_1 + \alpha_2 - 1)^{\frac{1}{2}} (\alpha_1 - \alpha_2 - 1)^{\frac{1}{2}}} - \frac{1}{(\alpha_1 + \alpha_2)^{\frac{1}{2}} (\alpha_1 - \alpha_2)^{\frac{1}{2}}}$$

and

$$\int_0^1 \frac{(\alpha_1 - \alpha) d\alpha}{(\alpha_1 - \alpha_2 - \alpha)^{3/2} (\alpha_1 + \alpha_2 - \alpha)^{\frac{1}{2}}} = \left( \frac{\alpha_1 + \alpha_2 - 1}{\alpha_1 - \alpha_2 - 1} \right)^{\frac{1}{2}} - \left( \frac{\alpha_1 + \alpha_2}{\alpha_1 - \alpha_2} \right)^{\frac{1}{2}} + 2 \log \left( \frac{(\alpha_1 - \alpha_2)^{\frac{1}{2}} + (\alpha_1 + \alpha_2)^{\frac{1}{2}}}{(\alpha_1 - \alpha_2 - 1)^{\frac{1}{2}} + (\alpha_1 + \alpha_2 - 1)^{\frac{1}{2}}} \right)$$

The first integral in (A2.4) has a square root singularity at  $\alpha = 0$  and at  $\alpha = 1$ ,  $\alpha_1 + \alpha_2 = 1$ . These can be mapped into points outside the range of integration by making the transformation

$$\alpha = 0.25 (2 + 3\zeta - \zeta^3) \tag{A2.6}$$

The double integral then becomes

$$- \int_{\beta_1}^{\beta_2} \int_{-1}^1 \frac{1.5 (\alpha_1 - \alpha) (1 - \zeta) F_{3,4}(\alpha, \beta) d\zeta d\beta}{c(\beta) (2 - \zeta)^{\frac{1}{2}} (\alpha_1 - \alpha_2 - \alpha)^{3/2} (\alpha_1 + \alpha_2 - \alpha)^{3/2}} \tag{A2.7}$$

Also since  $\alpha_1 + \alpha_2 = 1$  at  $\beta_2$  in Region 3 and at  $\beta_1$  in Region 4, the second integral in (A2.4) also has a square root singularity.

In Region 3 make the transformation

$$\beta = 0.25 [3\beta_2 + \beta_1 + (\beta_2 - \beta_1)(2\gamma_3 - \gamma_3^2)] \quad (\text{A2.8})$$

and this integral becomes

$$-\int_{-1}^1 \frac{f(1, \beta)}{2c(\beta)} \cdot \frac{(\beta_2 - \beta_1)(1 - \gamma_3) d\gamma_3}{(\alpha_1 + \alpha_2 - 1)^{\frac{1}{2}} (\alpha_1 - \alpha_2 - 1)^{\frac{1}{2}}} \quad (\text{A2.9})$$

which is regular.

In Region 4 make the transformation

$$\beta = 0.25 [3\beta_1 + \beta_2 + (\beta_2 - \beta_1)(2\gamma_4 + \gamma_4^2)] \quad (\text{A2.10})$$

and the integral becomes

$$-\int_{-1}^1 \frac{f(1, \beta)}{2c(\beta)} \cdot \frac{(\beta_2 - \beta_1)(1 + \gamma_4) d\gamma_4}{(\alpha_1 + \alpha_2 - 1)^{\frac{1}{2}} (\alpha_1 - \alpha_2 - 1)^{\frac{1}{2}}} \quad (\text{A2.11})$$

Hence,

$$\begin{aligned} I_{3,4} = & -\int_{\beta_2}^{\beta_1} \int_{-1}^1 \frac{1.5(\alpha_1 - \alpha)(1 - \zeta) F_{3,4}(\alpha, \beta) d\zeta d\beta}{c(\beta)(2 - \zeta)^{\frac{1}{2}} (\alpha_1 - \alpha_2 - \alpha)^{3/2} (\alpha_1 + \alpha_2 - \alpha)^{3/2}} + \int_{\beta_1}^{\beta_2} \frac{f(1, \beta) d\beta}{c(\beta)(\alpha_1 + \alpha_2)^{\frac{1}{2}} (\alpha_1 - \alpha_2)^{\frac{1}{2}}} \\ & + \int_{\beta_1}^{\beta_2} \frac{1}{c(\beta)} \left[ f_{\alpha}(1, \beta) - \frac{1}{2} f(1, \beta) \right] \left[ \left( \frac{\alpha_1 + \alpha_2 - 1}{\alpha_1 - \alpha_2 - 1} \right)^{\frac{1}{2}} - \left( \frac{\alpha_1 + \alpha_2}{\alpha_1 - \alpha_2} \right)^{\frac{1}{2}} \right. \\ & \left. + 2 \log \left( \frac{(\alpha_1 - \alpha_2)^{\frac{1}{2}} + (\alpha_1 + \alpha_2)^{\frac{1}{2}}}{(\alpha_1 - \alpha_2 - 1)^{\frac{1}{2}} + (\alpha_1 + \alpha_2 - 1)^{\frac{1}{2}}} \right) \right] d\beta \\ & + h(\beta). \end{aligned} \quad (\text{A2.12})$$

For Region 3,  $\beta_1 = 0$ ,  $\beta_2 = N[1]$  and  $h(\beta)$  is given by (A2.9).

For Region 4,  $\beta_1 = N[2]$ ,  $\beta_2 = 0$  and  $h(\beta)$  is given by (A2.11).

### APPENDIX III

#### *Aerofoil Polynomials.*

(a) *R.A.E. 101 - thickness/chord ratio 0.1.*

$$0 \leq \alpha \leq 0.28$$

$$\begin{aligned} f_1(\alpha) = & 0.061782 - 0.135607\alpha - 0.133082\alpha^2 \\ & + 0.738461\alpha^3 - 7.994151\alpha^4 + 31.611163\alpha^5 - 50.687233\alpha^6 \end{aligned}$$



$$0.28 \leq \alpha \leq 0.34$$

$$f_1(\alpha) = 18.046730 - 235.611250\alpha - 1155.471251\alpha^2 \\ - 2518.812502\alpha^3 + 2056.250002\alpha^4$$

$$0.34 \leq \alpha \leq 0.76$$

$$f_1(\alpha) = 0.272028 - 2.146999\alpha + 7.633440\alpha^2 \\ - 16.766700\alpha^3 + 21.219930\alpha^4 - 14.269058\alpha^5 \\ + 4.002758\alpha^6$$

$$0.76 \leq \alpha \leq 1.0$$

$$f_1(\alpha) = -0.035748 - 0.057645\alpha - 0.001233\alpha^2 \\ + 0.005197\alpha^3$$

(b) *R.A.E. 101 - 6 polynomial approximation.*

$$0 \leq \alpha \leq 0.12$$

$$f_1(\alpha) = 0.061782 - 0.136320\alpha - 0.0865456\alpha^2 - 0.194030\alpha^3$$

$$0.12 \leq \alpha \leq 0.3$$

$$f_1(\alpha) = -0.0315057 + 2.97501\alpha - 42.5912\alpha^2 + 304.424\alpha^3 \\ - 1208.75\alpha^4 + 2520.99\alpha^5 - 2165.80\alpha^6$$

$$0.3 \leq \alpha \leq 0.32$$

$$f_1(\alpha) = -0.002697 + 0.37605\alpha - 1.185\alpha^2$$

$$0.32 \leq \alpha \leq 0.62$$

$$f_1(\alpha) = 0.652986 - 7.03815\alpha + 33.5493\alpha^2 - 89.3162\alpha^3 \\ - 134.421\alpha^4 - 107.642\alpha^5 + 35.8206\alpha^6$$

$$0.62 \leq \alpha \leq 0.82$$

$$f_1(\alpha) = 6.04795 - 507.399\alpha + 1768.71\alpha^2 - 3279.59\alpha^3 \\ - 3409.64\alpha^4 - 1883.96\alpha^5 + 432.147\alpha^6$$

$$0.82 \leq \alpha \leq 1.0$$

$$f_1(\alpha) = -0.0260862 - 0.089711\alpha + 0.0341201\alpha^2 - 0.00775194\alpha^3$$

*N.B.* The polynomials given in (a) are a better approximation to R.A.E. 101 than the above and are the ones used in all the calculations except those for Table 3.

(c) *R.A.E. 103 - thickness/chord ratio 0.1.*

$$0 \leq \alpha \leq 0.36$$

$$f_1(\alpha) = 0.056254 - 0.105745\alpha - 0.053495\alpha^2 \\ - 0.106233\alpha^3 + 0.200182\alpha^4 - 0.562663\alpha^5$$

$$0.36 \leq \alpha \leq 0.42$$

$$f_1(\alpha) = -24.027736 + 247.803380\alpha - 956.018249\alpha^2 \\ + 1636.674998\alpha^3 - 1049.999999\alpha^4$$

$$0.42 \leq \alpha \leq 0.52$$

$$f_1(\alpha) = -274.634800 + 2973.909026\alpha - 12860.61416\alpha^2 \\ + 27763.82396\alpha^3 - 29920.85938\alpha^4 + 12876.04167\alpha^5$$

$$0.52 \leq \alpha \leq 0.80$$

$$f_1(\alpha) = 12.251779 - 107.979725\alpha + 399.043950\alpha^2 \\ + 790.318651\alpha^3 + 881.190451\alpha^4 - 523.746444\alpha^5 \\ + 129.619017\alpha^6$$

$$0.80 \leq \alpha \leq 1.0$$

$$f_1(\alpha) = -0.030909 - 0.104182\alpha + 0.038922\alpha^2 \\ - 0.008703\alpha^3$$

TABLE 1

*A Comparison of Values of  $C_p$  on Wing 1, Mach 1.2 when using 10 Point and 20 Point Gaussian Integration.*

X	Y	$C_p$ 10 pt. integration	$C_p$ 20 pt. integration	%
0.05	0	0.186401	0.186401	0
0.1	0	0.113438	0.113438	0
0.2	0	0.049949	0.049949	0
0.3	0	0.005426	0.004862	11.6
0.4	0	-0.030530	-0.030041	1.6
0.5	0	-0.049627	-0.049098	1.1
0.6	0	-0.060656	-0.061616	-1.6
0.7	0	-0.067615	-0.067536	0.1
0.8	0	-0.067488	-0.068101	-0.9
0.9	0	-0.066836	-0.068098	-1.9
0.975	0	-0.066871	-0.068194	-1.9
0.025	0.3	-0.025085	-0.025664	-2.3
0.05	0.3	-0.032150	-0.032236	-0.3
0.1	0.3	-0.048414	-0.048524	-0.2
0.2	0.3	-0.079968	-0.079934	0.4
0.3	0.3	-0.106006	-0.106655	-0.6
0.4	0.3	-0.107039	-0.107121	-0.07
0.5	0.3	-0.103536	-0.102987	-0.5
0.6	0.3	-0.095017	-0.095814	-0.8
0.7	0.3	-0.086464	-0.086970	-0.6
0.765	0.3	-0.082921	-0.081963	1.2
0.775	0.3	-0.070798	-0.069800	1.4
0.8	0.3	-0.049676	-0.049928	-0.5
0.9	0.3	-0.005350	-0.005872	-8.9
0.975	0.3	0.039719	0.039204	1.1

TABLE 2

*A Comparison of Exact and Calculated Values for a Simple Chordwise Integration.*

$\theta$	$\delta$	$I^*$ exact value	$I^*$ numerical value 10 pt. integration	%
85°	0.0038125	2.82449	2.82451	0.0007
87°	0.0013714	3.33568	3.33571	0.0009
88°	0.0006094	3.74127	3.74120	-0.002
89°	0.0001523	4.43450	4.43448	-0.0005

TABLE 3

*A Comparison of Values of  $C_p$  on Wing 1, Mach 1.2 for two Different Approximations to the Thickness Distribution.*

$X$	$Y$	4 polynomial fit $C_p$	6 polynomial fit $C_p$	%
0.05	0	0.186401	0.186418	0.009
0.1	0	0.113438	0.113427	-0.01
0.2	0	0.0499487	0.0499487	0
0.3	0	0.00542626	0.00486795	-10.3
0.4	0	-0.0305297	-0.0296780	-2.8
0.5	0	-0.0496268	-0.0492956	-0.7
0.6	0	-0.0606557	-0.0606683	0.0.2
0.7	0	-0.0676152	-0.0681522	0.8
0.8	0	-0.0674879	-0.0683206	1.2
0.9	0	-0.0668355	-0.0667964	0.06
0.975	0	-0.0668709	-0.0670641	0.29
0.025	0.3	-0.0250850	-0.0250375	-0.2
0.05	0.3	-0.0321496	-0.0321535	0.07
0.1	0.3	-0.0484141	-0.0482865	-0.3
0.2	0.3	-0.0799677	-0.0800282	0.08
0.3	0.3	-0.106006	-0.106999	0.9
0.4	0.3	-0.107039	-0.106769	-0.25
0.5	0.3	-0.103536	-0.103485	-0.05
0.6	0.3	-0.0950165	-0.0951855	0.2
0.7	0.3	-0.0864637	-0.0867300	0.3
0.765	0.3	-0.0829205	-0.0820828	-1.0
0.775	0.3	-0.0707977	-0.0698637	-1.3
0.8	0.3	-0.0496764	-0.0496614	-0.3
0.9	0.3	-0.00535026	-0.00490073	-8.4
0.975	0.3	0.0397188	0.0400351	0.8

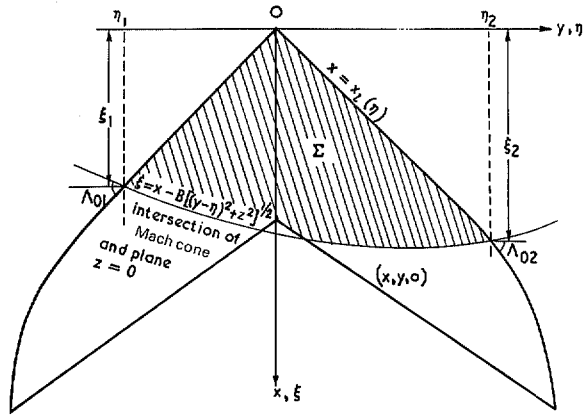


FIG. 1. Area of integration for a general point  $(x, y, z)$ .

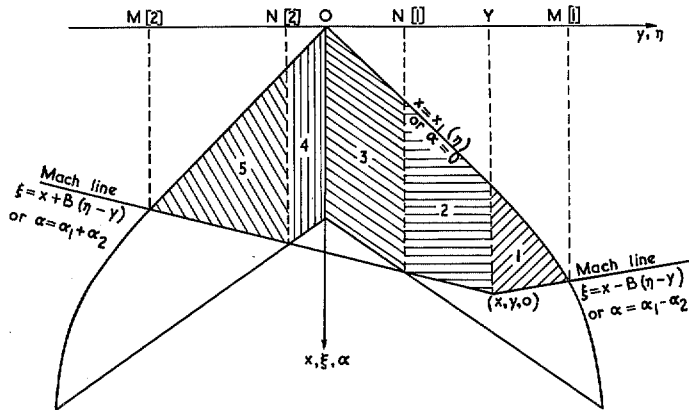


FIG. 2. Regions of integration for point  $(x, y, 0)$ .

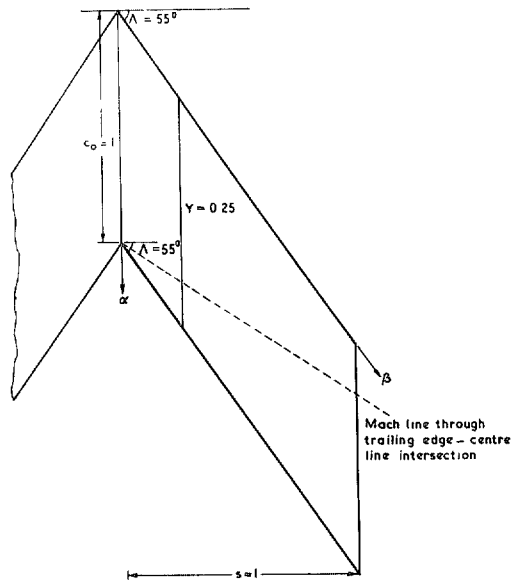


FIG. 3. Plan of Wing 1. R.A.E. 101 section  $t/c = 0.054$ .

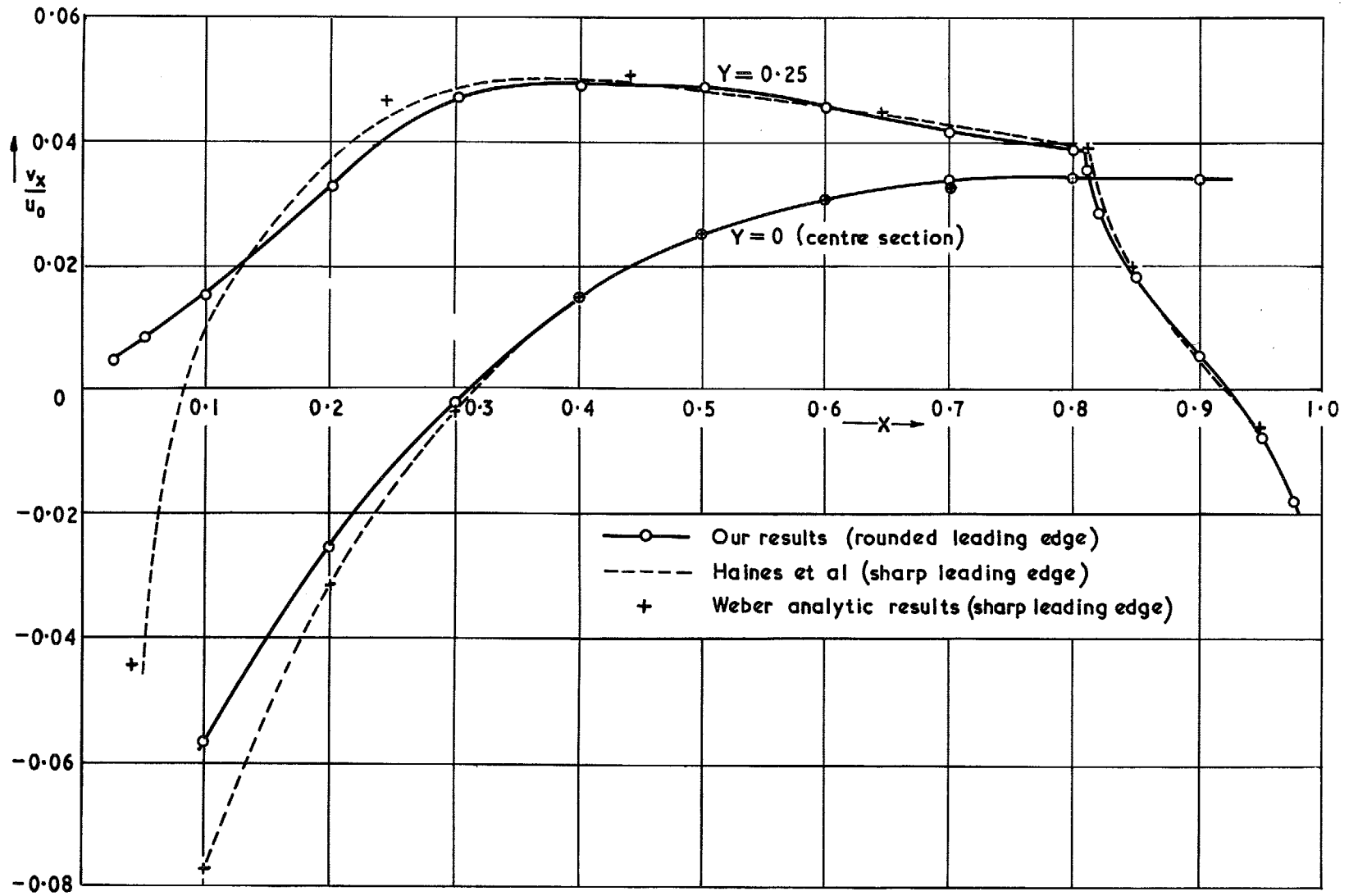


FIG. 4. Wing 1 – a comparison with the results of Haines, Rollins and Osborne, Mach 1.2.

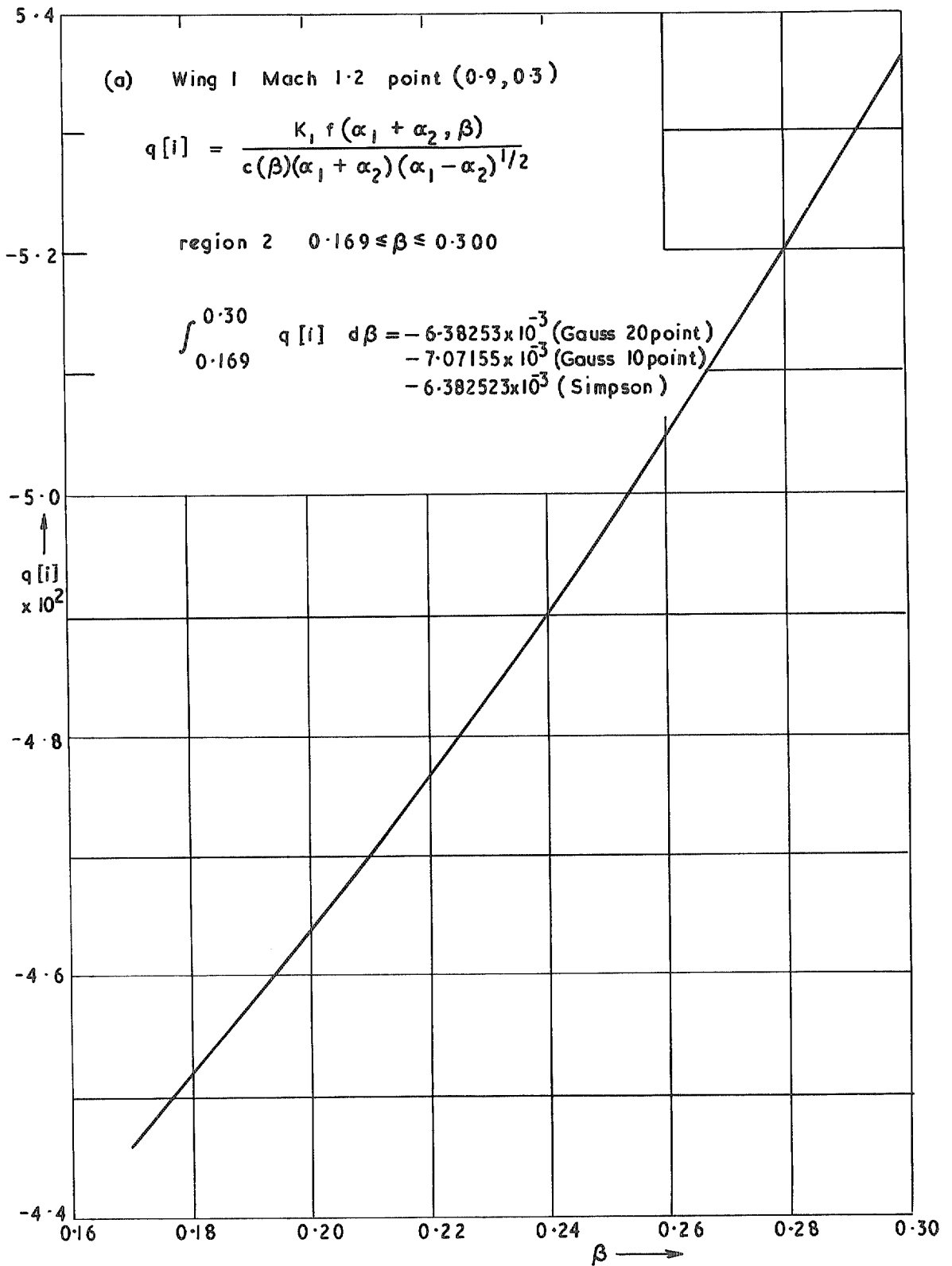


FIG. 5a. Values of various integrands in equation (3.7).

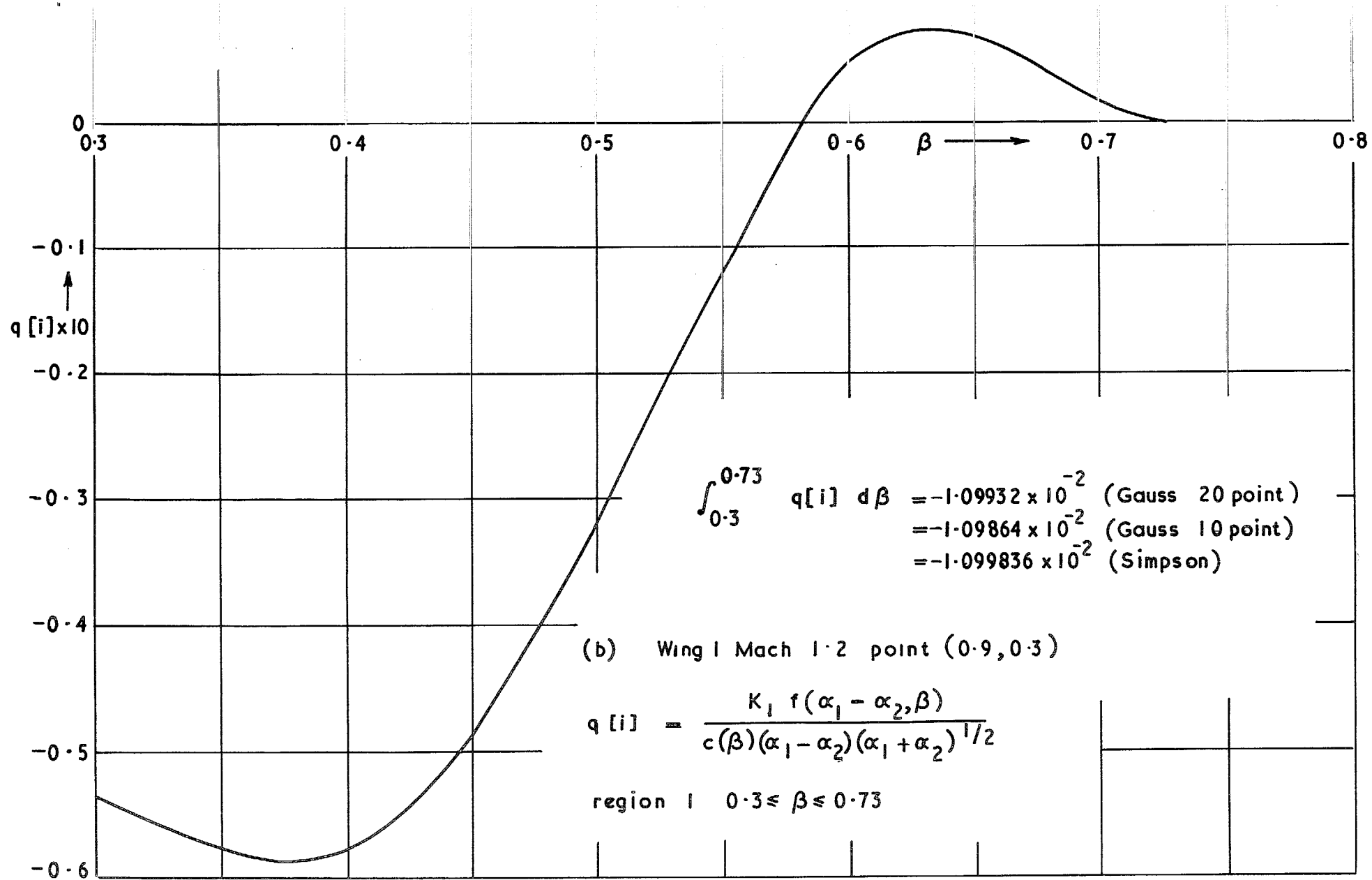


FIG. 5b. Values of various integrands in equation (3.7).



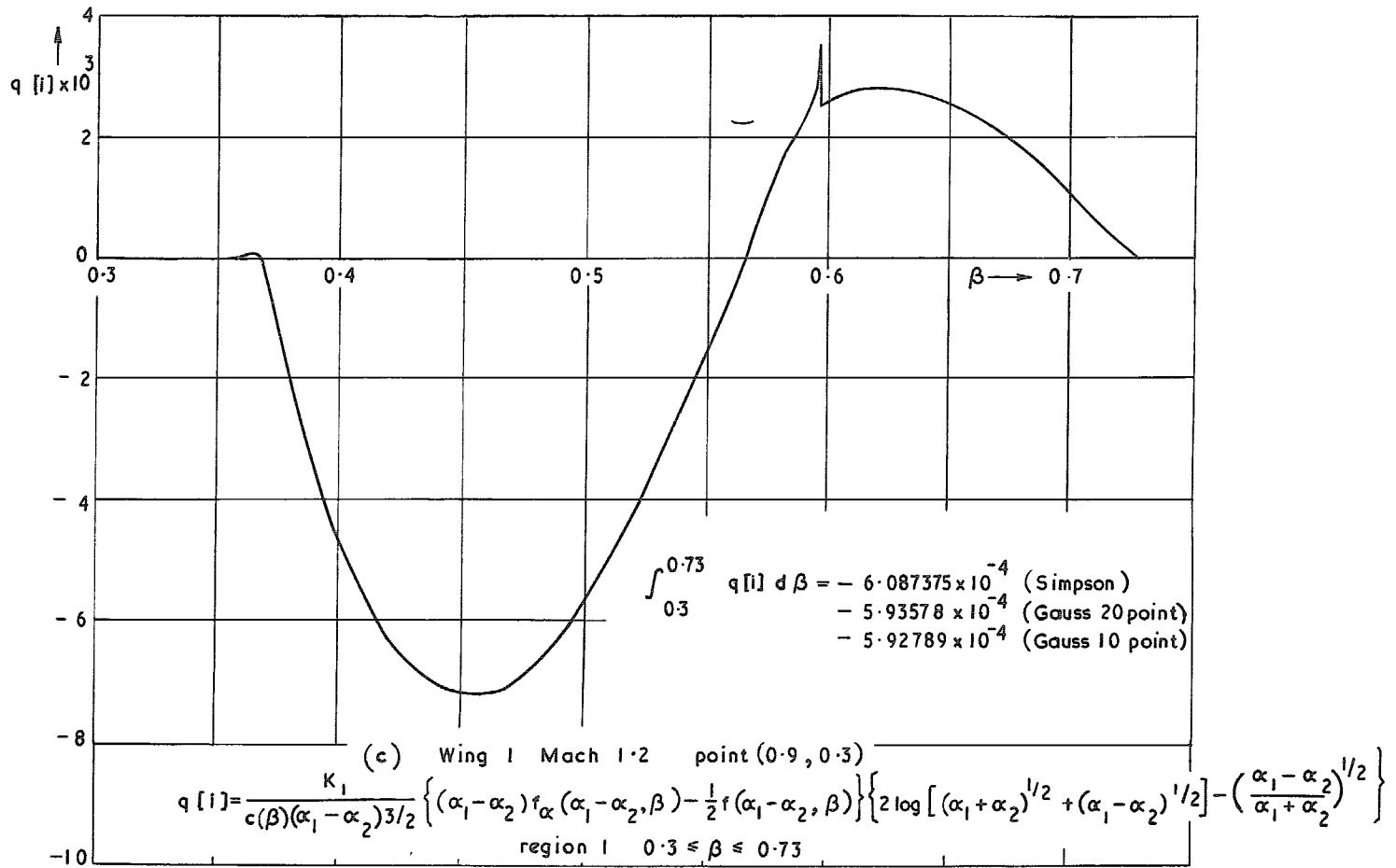


FIG. 5c. Values of various integrands in equation (3.7).

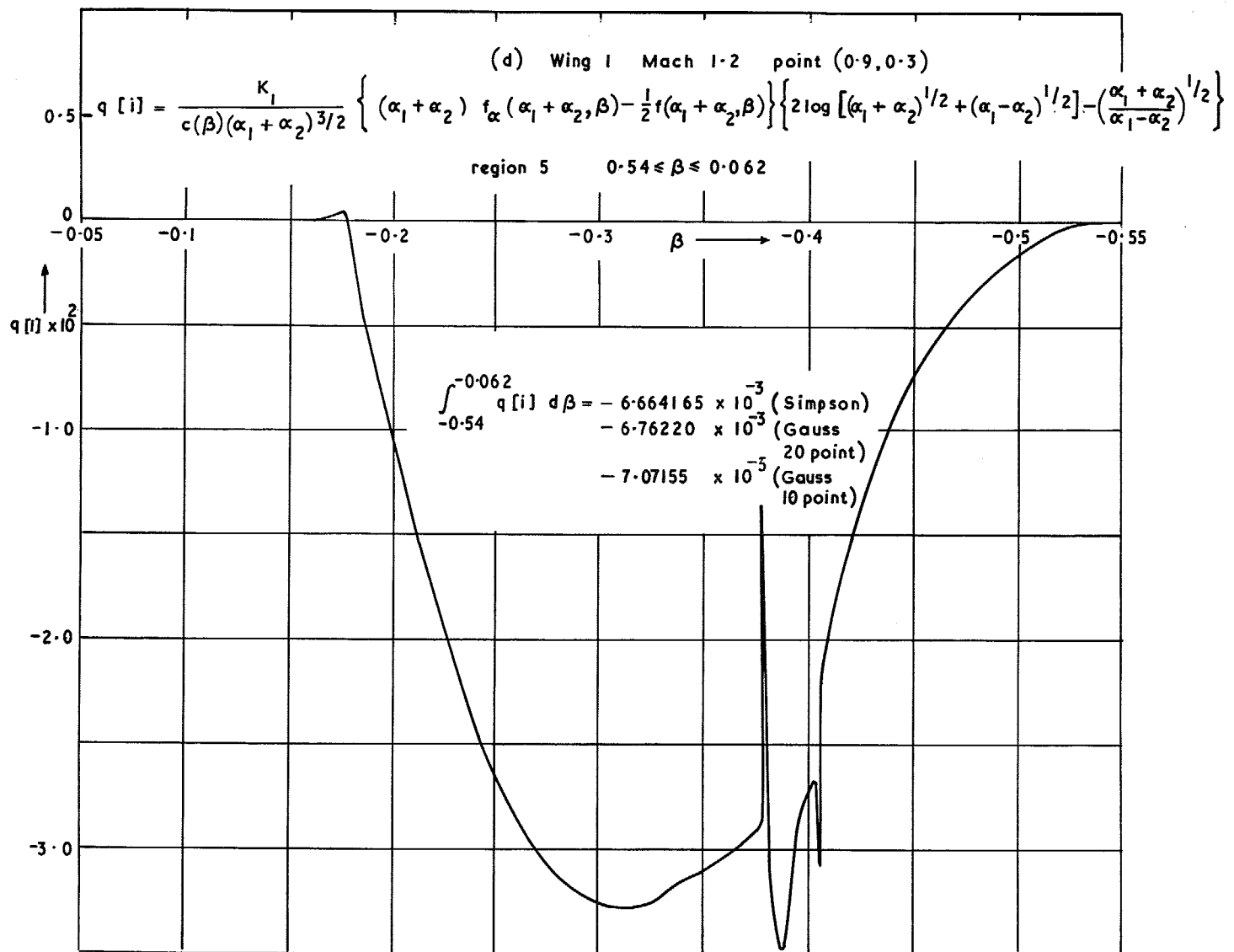


FIG. 5d. Values of various integrands in equation (3.7).

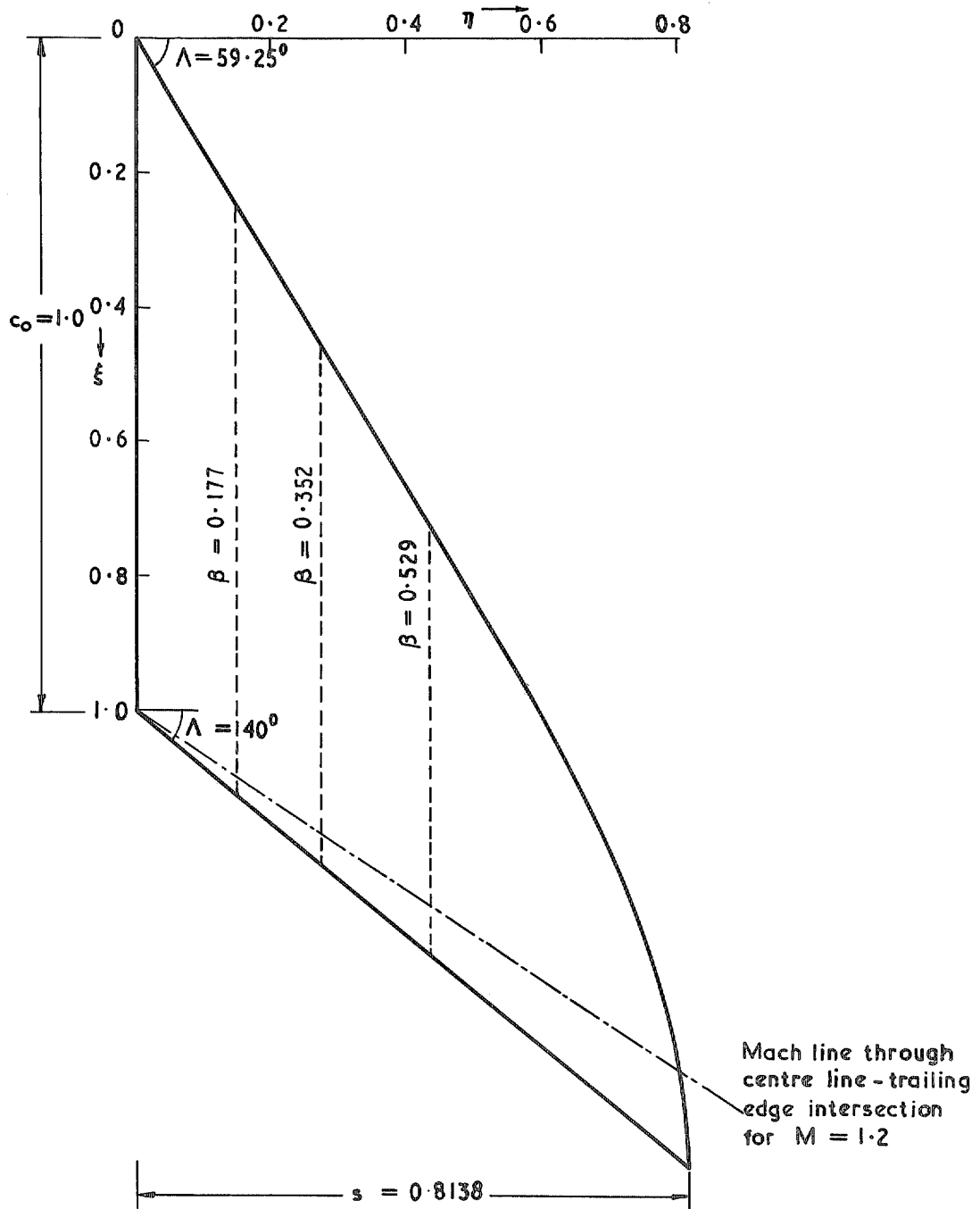


FIG. 6. Plan of Wing 2 R.A.E. 101 section  $t/c = 0.06$ .

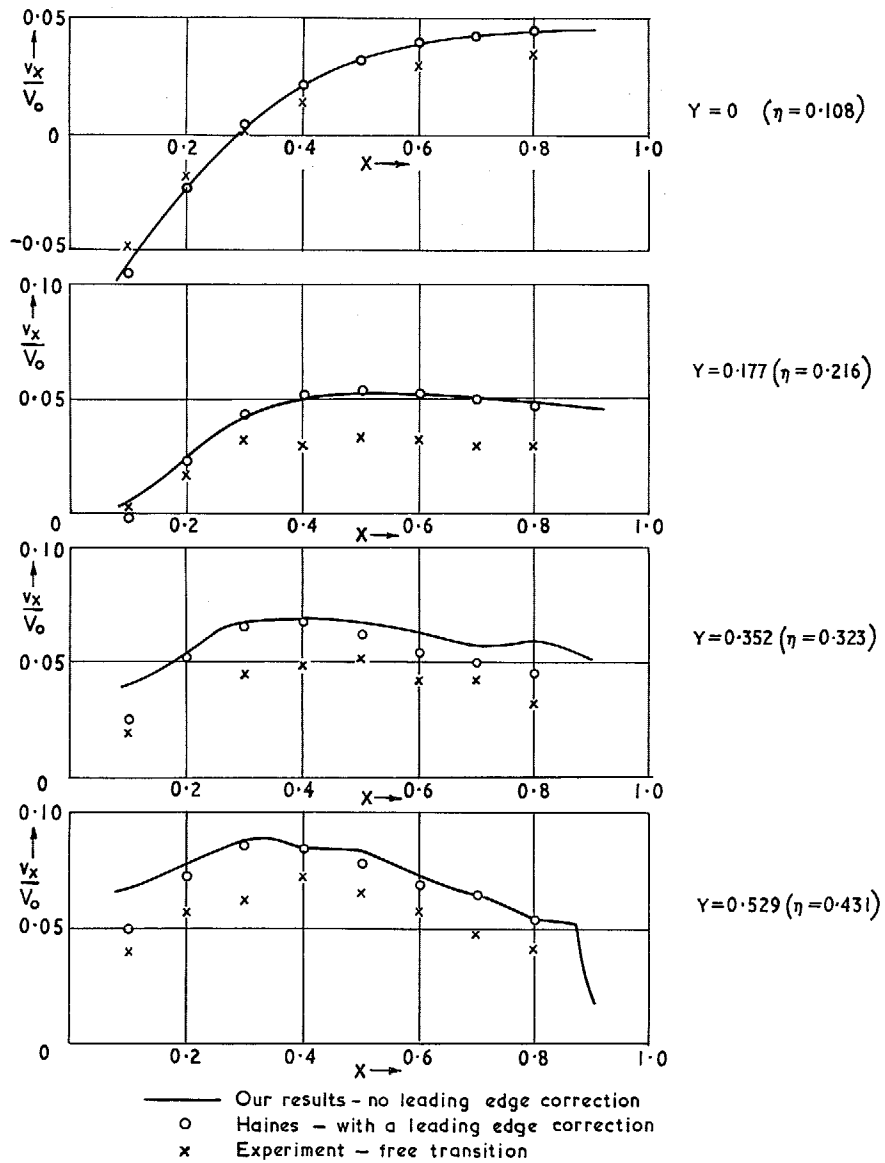


FIG. 7. A comparison with experiment results and those of Haines *et al*, wing B Wing 2 Mach 1.2.

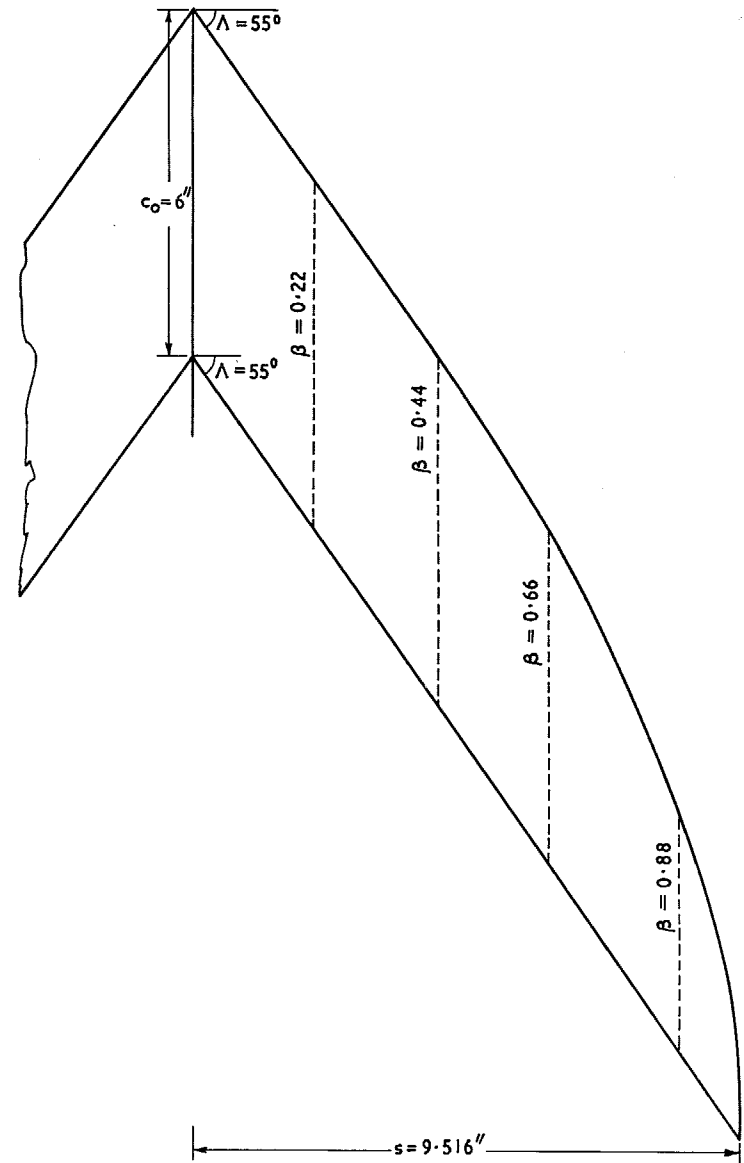


FIG. 8. Plan of Wing 3 N.P.L. 55° Wing R.A.E. 103 section  $t/c = 0.06883$ .

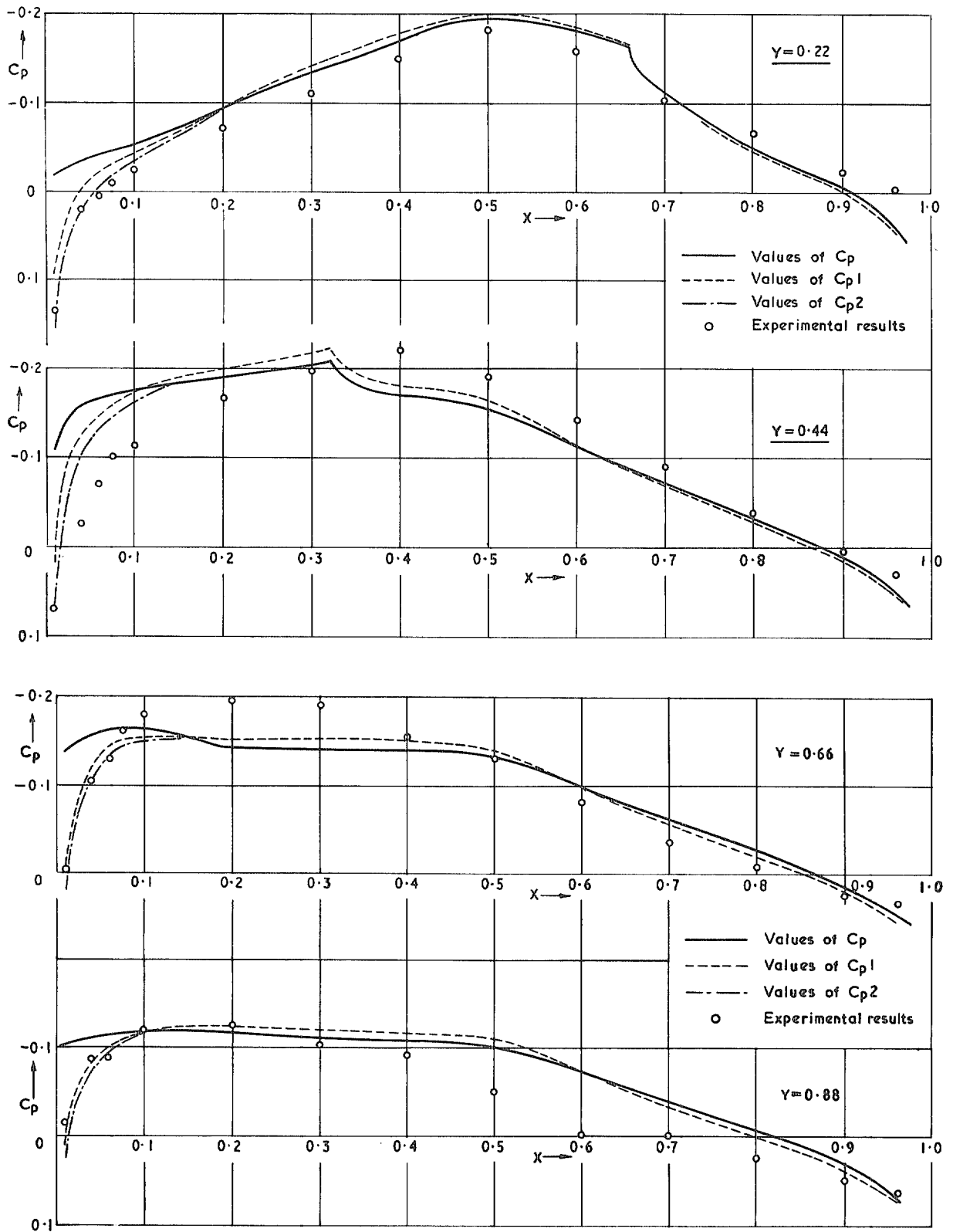


FIG. 9. A comparison of calculated and experimental results Wing 3 Mach 1.1.

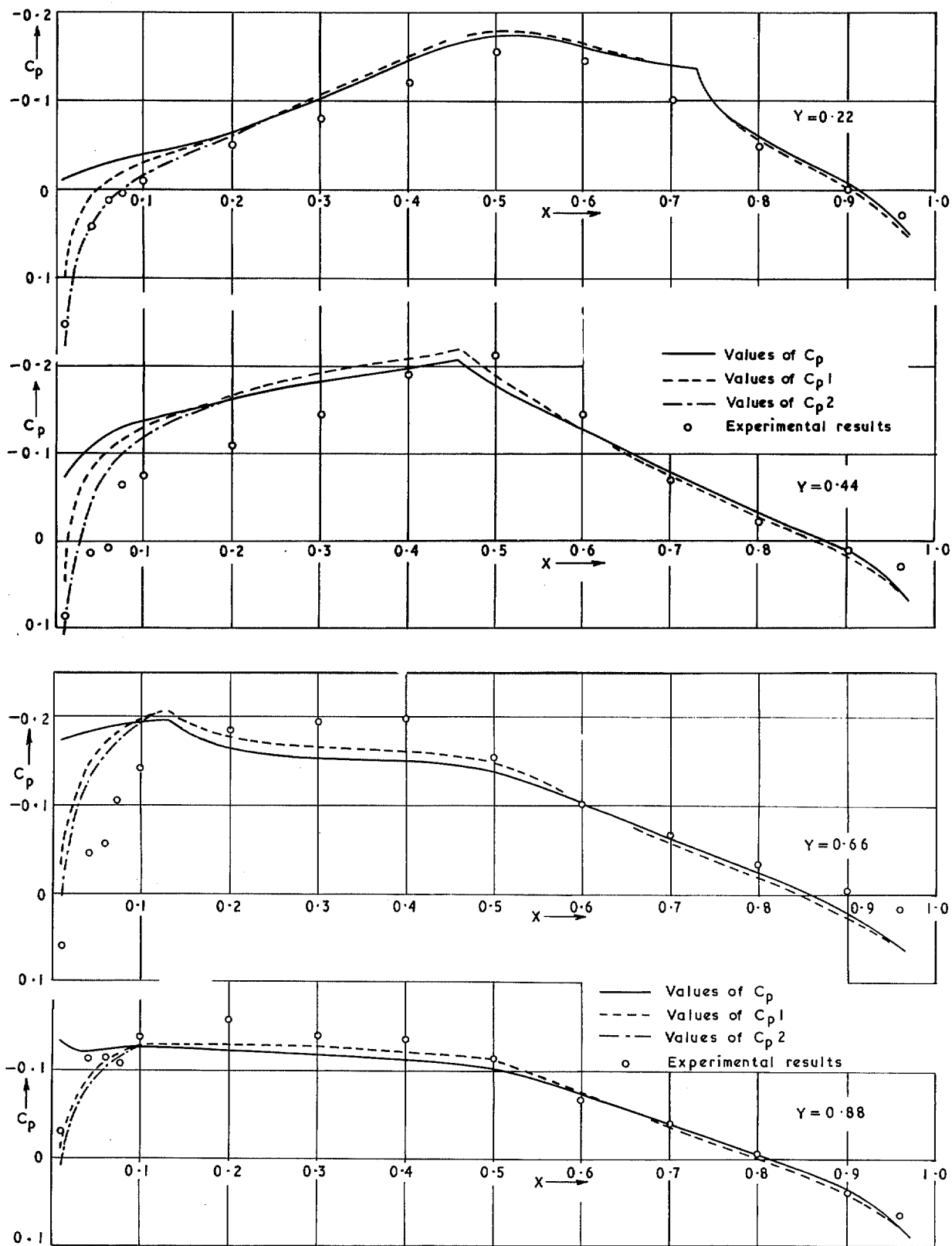


FIG. 10. A comparison of calculated and experimental results Wing 3 Mach 1.2.

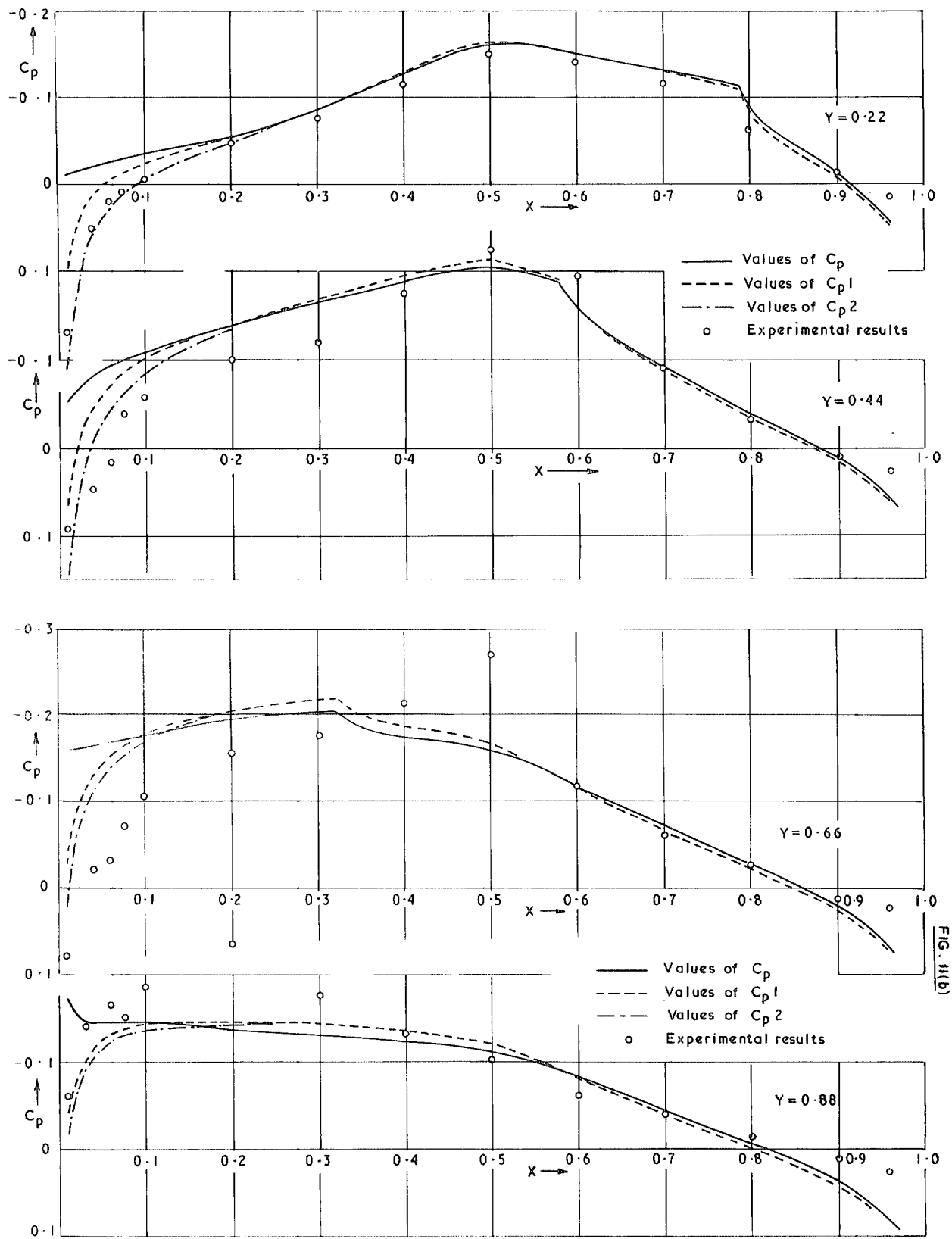


FIG. 11. A comparison of calculated and experimental results Wing 3 Mach 1.3.

28 359  
FIG. 11(b)

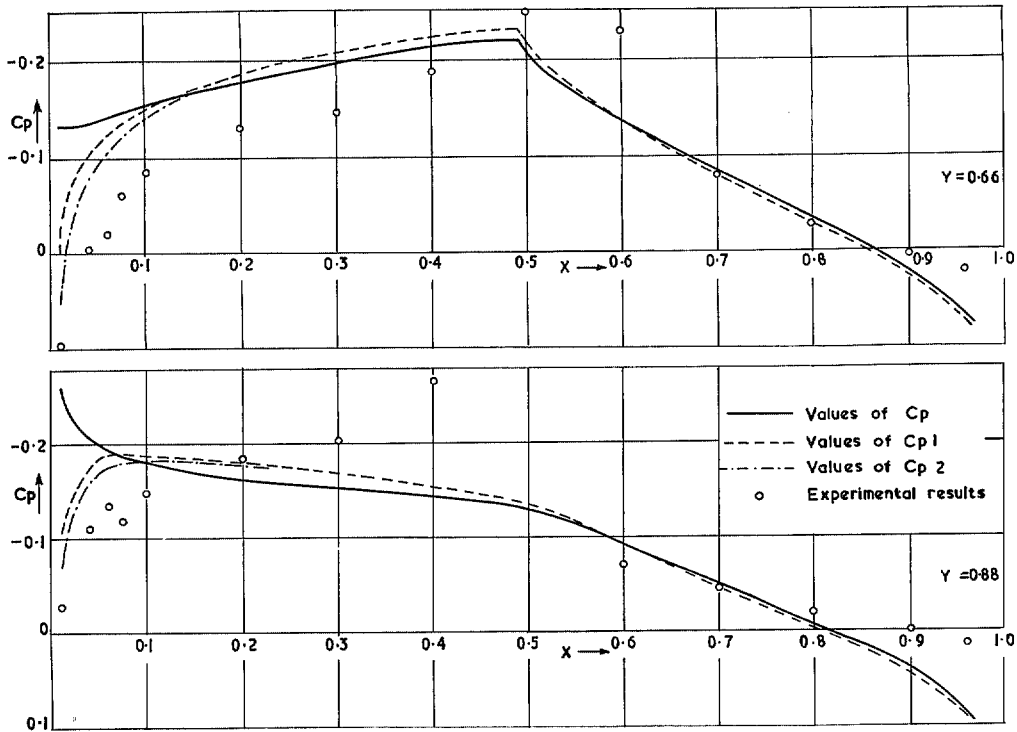
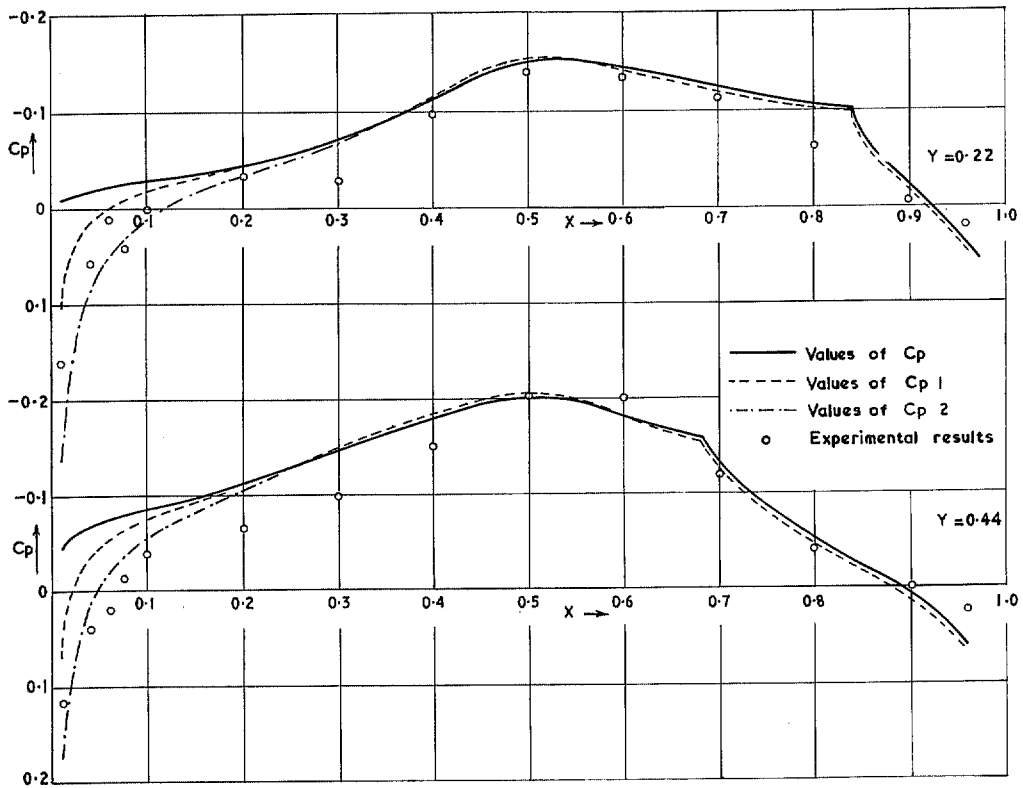


FIG. 12. A comparison of calculated and experimental results Wing 3 Mach 1.4.



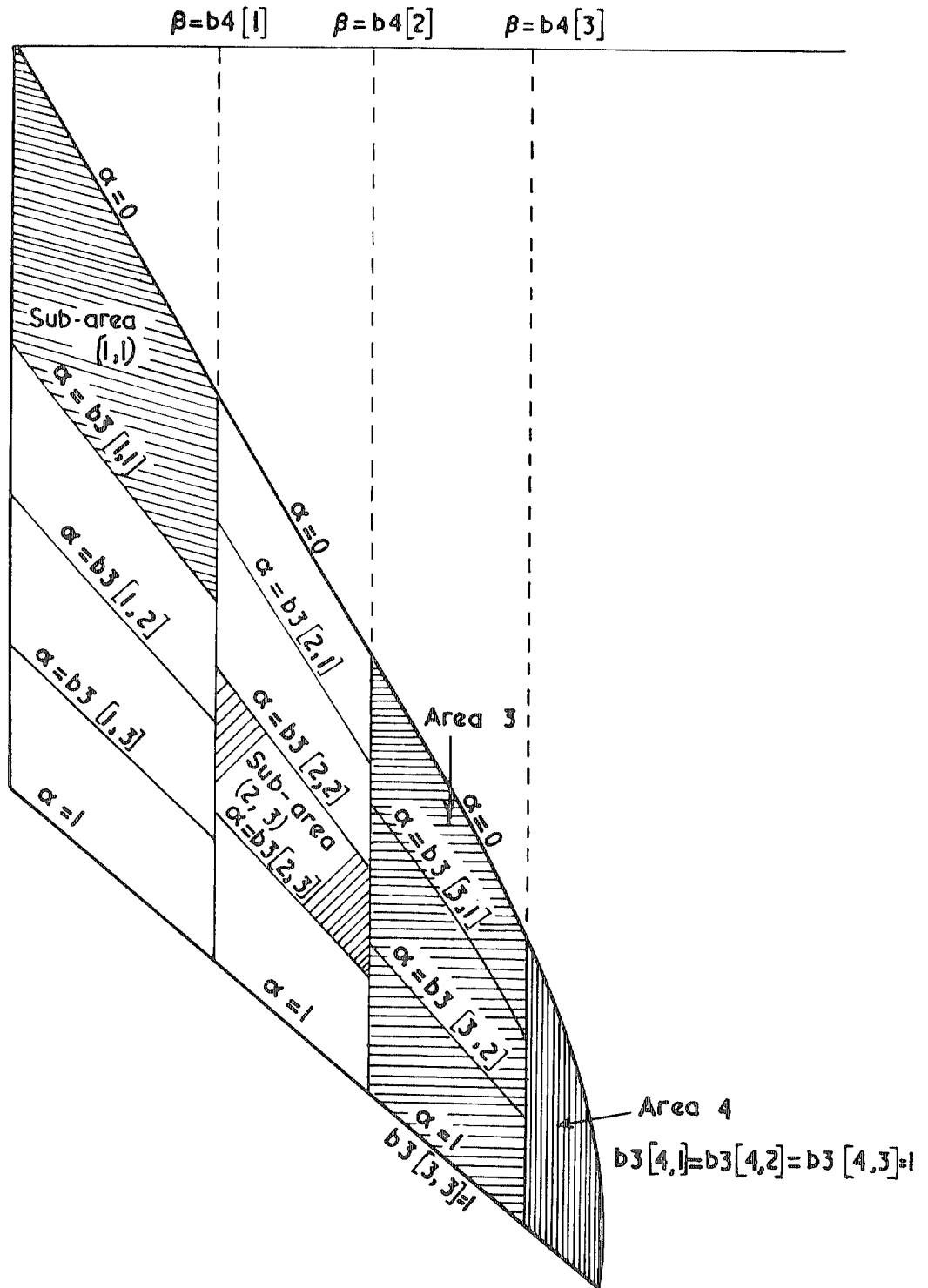


FIG. 13. Diagram showing how a wing may be split into areas and sub-areas for defining thickness.

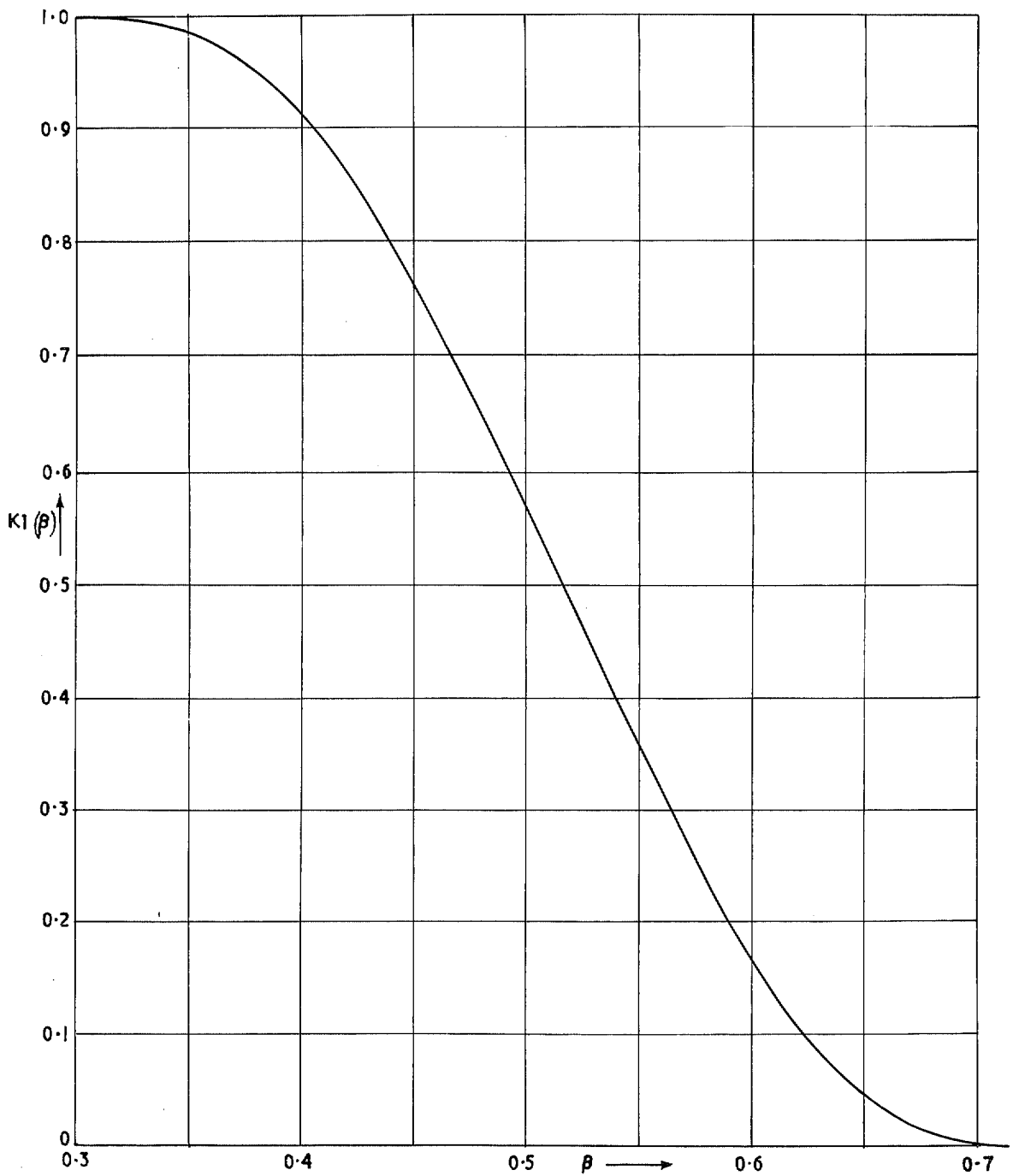


FIG. 14. Typical graph of  $K1(\beta)$  for region 1.

*C. Crown copyright 1968*

Published by  
HER MAJESTY'S STATIONERY OFFICE

To be purchased from  
49 High Holborn, London W.C.1  
423 Oxford Street, London W.1  
13A Castle Street, Edinburgh 2  
109 St. Mary Street, Cardiff CF1 1JW  
Brazenose Street, Manchester 2  
50 Fairfax Street, Bristol 1  
258-259 Broad Street, Birmingham 1  
7-11 Linenhall Street, Belfast BT2 8AY  
or through any bookseller